

# Morphological and Physiological Properties of Geniculate W-Cells of the Cat: a Comparison With X- and Y-Cells

L. R. STANFORD, MICHAEL J. FRIEDLANDER, AND  
S. MURRAY SHERMAN

*Department of Neurobiology and Behavior, State University of New York,  
Stony Brook, New York 11794*

## SUMMARY AND CONCLUSIONS

1. We used intracellular recording and iontophoresis of horseradish peroxidase (HRP) to study the morphology of physiologically characterized W-cells in the cat's lateral geniculate nucleus. Morphological study was limited to light microscopy. Our data from 20 W-cells of the C-laminae were compared to analogous data we previously published for geniculate X- and Y-cells of the A- and C-laminae.

2. W-cell somata were comparable in size to X-cell somata, and both classes had smaller somata than did Y-cells.

3. W-cell dendrites were thin and usually varicose or beaded; some had complex, stalked appendages or clusters of appendages near dendritic branch points. X-cell dendrites were also thin and often had clustered appendages. However, Y-cell dendrites were thick and generally appendage free.

4. W-cell dendritic arbors were slightly more extensive than those of X- and Y-cells. While Y-cell arbors exhibited approximately spherical symmetry, those of W-cells were elongated parallel to the geniculate laminar borders and those of X-cells were elongated perpendicular to these borders. Some dendrites of every W- and Y-cell crossed laminar borders, whereas the dendrites of every X-cell were always confined to a single lamina.

5. W-cell axons were thinner than those of X-cells, and X-cells had thinner axons than did Y-cells. All three cell classes commonly had axons that, en route to cerebral cortex, innervated the perigeniculate nucleus

via collateral branches. Occasionally, intrageniculate axon collaterals (i.e., within the main geniculate laminae) were seen for W-, X-, and Y-cells.

6. The morphological features of W-cells clearly indicate that these neurons represent a class different from X- or Y-cells. Furthermore, despite the physiological and morphological heterogeneity we observed among these W-cells, we saw no clear evidence that they comprise more than a single neuronal class. More data are needed to determine whether or not these neurons form a single class.

7. The striking morphological differences among geniculate W-, X-, and Y-cells suggest corresponding differences in neuronal processing and synaptic integration. Functional differences among the W-, X-, and Y-cell pathways are thus probably not limited to and solely determined by retinal processing but are further elaborated by these geniculate neurons.

8. We have speculated how the different morphological features of geniculate W-, X-, and Y-cells might relate to their different physiological properties and functional roles. The Y-cells seem most responsive to synaptic input and are thought to play a key role in basic form analysis. Their thick, appendage-free dendrites may contribute to their efficient synaptic transmission. W- and X-cells have dendritic appendages (that are probably postsynaptic specializations), dendritic constrictions, and thinner dendrites. These dendritic features are consistent with

the apparently less efficient synaptic transmission through these neurons. Finally, X-cell arbors, which extend along "projection lines," are suited for maximum convergence of synaptic inputs from the smallest representation of visual field, and this might relate to the observation that X-cells are particularly concerned with fine spatial detail. The elongation of W-cell dendrites across projection lines suggests convergence of inputs from an extensive representation of visual space, a property consistent with the larger, more diffuse receptive fields of these neurons.

## INTRODUCTION

Enroth-Cugell and Robson (10) first demonstrated that retinal ganglion cells in the cat contain two distinct functional classes, called X- and Y-cells. Since that time, a great deal of attention has been focused on the parallel pathways from the retina through the lateral geniculate nucleus to the visual cortex. We currently recognize at least three such pathways, the W-, X-, and Y-cell pathways. These seem to be organized in parallel, functionally distinct circuits with limited overlap (48).

Some of the physiological differences among these neuronal classes in the retina and lateral geniculate nucleus are as follows (for recent reviews, see Refs. 33, 40, 44, 45, 48, 49). 1) W-cell axons conduct more slowly than do X-cell axons, which in turn conduct more slowly than do Y-cell axons. 2) W-cells are considerably less sensitive to visual stimuli than are either X- or Y-cells. 3) X-cells tend to display fairly linear spatial and temporal summation of visual stimuli, whereas Y-cells exhibit nonlinear response components; some W-cells are linear in this regard, while others are nonlinear. 4) Y-cells are most sensitive to lower spatial frequencies, and X-cells are most sensitive to higher ones; W-cells are rather insensitive to all spatial frequencies but respond relatively better to lower ones. 5) X-cells tend to have smaller receptive fields than do Y-cells; W-cells tend to have the largest receptive fields, but some are as small as those of Y-cells. Other differences have also been noted.

The above-mentioned properties represent physiological distinctions. Attention has been recently focused on anatomical differences among these pathways. For instance, the

three pathways involve different divisions of the lateral geniculate nucleus (5, 8, 29, 53). The A-laminae contain a mixture of X- and Y-cells. The C-laminae contain a nearly pure population of W-cells except for Y-cells and perhaps rare X-cells located at the dorsal tier of lamina C. The medial interlaminar nucleus is comprised mainly of Y-cells, although some W- and X-cells may also be found there.

We have been interested in the morphological substrates of these pathways at the single neuron level and have focused on geniculate cells for this approach. We used micropipettes filled with horseradish peroxidase (HRP) to record these cells and identify each as a W-, X-, or Y-cell. We then penetrated the cell to iontophorese HRP into it for subsequent morphological analysis of the physiologically identified neuron. We used this technique to demonstrate characteristic morphological differences between geniculate X- and Y-cells (14, 15). In the present study we extend this to W-cells of the C-laminae. From these data we can demonstrate significant morphological differences among the three physiological classes, and these differences indicate that different functional processing continues for each of these pathways in the lateral geniculate nucleus. A preliminary report of some of these data from W-cells has recently appeared (46).

## METHODS

### *General preparation*

Adult cats (2.0–4.0 kg) were used for all experiments. Cats were initially anesthetized with 4% halothane and a 1:1 mixture of N<sub>2</sub>O/O<sub>2</sub>. Following anesthetic induction, a 0.4-mg dose of atropine was administered subcutaneously to prevent excessive respiratory secretion, a femoral vein was cannulated, the trachea was intubated, and a long-lasting local anesthetic (Deltacaine) was applied intra-aurally. The cat was then placed in a stereotaxic head holder. Paralysis was induced with 5 mg of gallamine triethiodide and maintained on a continuous intravenous infusion of paralytic agents (3.6 mg/h of gallamine triethiodide, 0.7 mg/h of *d*-tubocurarine, and 6 ml/h of 5% lactated Ringer solution). During the ensuing surgical manipulations the animal was artificially ventilated with 1% halothane in a 70/30 N<sub>2</sub>O/O<sub>2</sub> mixture. Expired CO<sub>2</sub> was monitored and kept near 4%, and body temperature was maintained between 37.5 and 38°C by a feedback-controlled electric-

blanket system. After the completion of all surgical manipulations and throughout the recording session, the 70/30 mixture of N<sub>2</sub>O/O<sub>2</sub> was given without halothane. All wound margins and pressure points were periodically infused with local anesthetic.

### Visual stimulation

Solutions of 1% atropine (to maintain pupillary dilation) and 2.5% phenylephrine (to retract the nictitating membrane) were applied to the eyes, and contact lenses were placed on the corneas. The lenses were chosen by retinoscopy to focus the retinas on the visual stimuli located on a plotting screen or cathode-ray tube.

The optic disks of both eyes were projected onto the plotting screen by the method of Fernald and Chase (12), which allowed us to determine the position of the receptive fields of our injected cells relative to the area centralis. Sanderson's (43) retinotopic maps were then used to correlate the recovered cells with receptive-field position within the lateral geniculate nucleus. Adequate spacing ( $\geq 1$  mm) of our injections within the nucleus ensured that subsequent identification was unambiguous.

Receptive fields were mapped with bright or dark spots on the plotting screen. For most cells, a counterphased, vertically oriented, sine-wave grating was generated on a cathode-ray tube to determine the cell's spatial summation properties. A cell was considered to sum linearly if it responded mainly at the fundamental counterphase frequency and had a demonstrable "null point" (i.e., a position of the grating pattern that elicited no response). A nonlinear response occurred at twice the fundamental counterphase frequency (second harmonic or doubling response) and exhibited no demonstrable null point. For this test, the spatial frequency, spatial phase, and temporal frequency (counterphase rate) were continuously variable. Contrast (defined as  $(L_{\max} - L_{\min}) / (L_{\max} + L_{\min})$ , where  $L_{\max}$  and  $L_{\min}$  are, respectively, the maximum and minimum luminance values across the grating) was also continuously variable between 0 and 0.8. Mean illumination ( $1/2(L_{\max} + L_{\min})$ ) was constant at 38 cd/m<sup>2</sup>.

### Electrophysiology

**ELECTRICAL STIMULATION.** A pair of insulated, tungsten-wire electrodes (exposed tip length approximately 0.5 mm) was used for bipolar, electrical stimulation of the optic chiasm. These electrodes were positioned in Horsley-Clarke coordinates at 14.5 mm anterior and 2.0 mm lateral on each side, and they were slowly lowered through the brain to straddle the optic chiasm. Final electrode position (usually 20–23 mm below the cortical surface) was determined by the maximal light-evoked response recorded differentially be-

tween the two electrodes. The electrodes were cemented into place at this position. Orthodromic activation of geniculate neurons was accomplished by delivering current pulses between these electrodes (0.01–0.1 ms, 1–3 mA). In some experiments, similar electrical stimuli were delivered to an array of four stimulating electrodes placed in visual cortex (approximately 1–4 mm below the surface) to effect antidromic or transynaptic activation of geniculate neurons. Transynaptic activation was defined by the criteria of Bishop et al. (2) for both optic chiasm and cortical stimulation. For cortical stimulation, antidromic activation was identified by little or no variability in the latency of the evoked spike and by the ability of an orthodromically traveling action potential to cancel the evoked spike (antidromic collision test). For all forms of electrical stimulation, latency was taken as the delay between the onset of the stimulus artifact and the "foot" of the evoked action potential. For transynaptic latencies, a number of responses were superimposed on a storage oscilloscope, and both the mode and range of latencies were measured. In this paper we shall refer only to the modal latencies. These were typically the midpoint of the latency range.

**ELECTROPHYSIOLOGICAL RECORDING.** Recording electrodes were glass micropipettes that were backfilled with a solution of 2–5% HRP (Sigma type VI) in 0.2 M KCl and 0.05 M Tris. The KCl-Tris solution was buffered to a pH of 7.6 and passed through a 0.05- $\mu$ m membrane filter. We then beveled the electrodes to an impedance of 80–120 M $\Omega$  at 100 Hz. This corresponded to a tip diameter of 0.2–0.5  $\mu$ m, as estimated from scanning electron micrographs. The electrodes were inserted into the brain through a hydraulically sealed chamber. A DC amplifier with bridge balancing and internal current-injection circuitry was used for all recording. The internal current-injection circuitry was externally gated.

Geniculate neurons were first studied and classified extracellularly using a battery of physiological tests and measurements. These included response latency to optic chiasm and visual cortex stimulation; briskness of response to visual targets; receptive-field size and position; sign (on or off) of the receptive-field center; ocular dominance; linearity of spatial summation to counterphased, sine-wave gratings; strength of inhibitory surround; response to fast-moving targets; and the tonic or phasic nature of the response to sustained stimulation of the receptive-field center. The primary criteria for identifying a neuron as a W-cell were a long response latency to optic chiasm stimulation, poor ("sluggish") responses to visual stimulation, and responses, when present, only to sine-wave gratings of relatively high contrast ( $>0.2$ ) and low spatial ( $<0.5$  cycles/deg) frequency. Since,

in the laminated portion of the lateral geniculate nucleus, W-cells have been found only in the C-laminae, we limited our injections to this region. It should be noted that the long response latencies of W-cells to optic chiasm stimulation could be due either to monosynaptic input from slowly conducting optic tract input or to multisynaptic input via midbrain (or other) pathways that innervate the C-laminae (18, 50). Our methods could not distinguish between these alternatives. Electrode position within the C-laminae could be determined by the pattern of ocular dominance changes seen as the electrode traversed the more dorsal A-laminae. Some of the W-cells encountered in the C-laminae were poorly responsive to visual stimuli and, therefore, had receptive fields whose borders were difficult to define; indeed, some were unresponsive to the visual stimuli we used. However, we determined the receptive-field positions of responsive C-laminae cells (all Y-cells and most W-cells) and A-laminae cells encountered in a penetration before one of these poorly responsive cells was recorded and injected with HRP. These other receptive-field locations permitted us to locate the filled cell in histological material with the aid of Sanderson's (43) retinotopic maps of the lateral geniculate nucleus.

After extracellular classification, the electrode was slowly advanced until the electrical effects of mechanical contact with the cellular membrane were evident. These effects included an increase in the low-frequency content of the recorded signal and increased spike amplitude. Brief (50–100 ms) depolarizing current pulses (1–3 nA) were then used to penetrate the cell. Impalement was indicated by a rapid 30- to 70-mV drop in the DC potential, large positive monophasic action potentials, and the presence of subthreshold synaptic potentials. During visual stimulation, the evoked burst of action potentials typically rode on a slow depolarizing wave. After penetration, the cells' electrophysiological properties were rechecked to ensure that the penetrated cell and the extracellularly recorded neuron were the same. At this point, HRP was iontophoresed into the cell with depolarizing current pulses (3–4 Hz, 70% duty cycle  $\leq$  10 nA). We interrupted the injection at frequent intervals to ensure that the cell still displayed a stable resting potential. Loss of 50% of the initial rest potential was cause for termination of the injection procedure. Otherwise, iontophoresis continued for 5–10 min, after which time the micropipette was withdrawn rapidly. This terminated the penetration and a new penetration was started at least 1 mm distant.

### *Histology*

At least 1 h after the final injection and <24 h after the first, the cats were given 100 mg of

sodium pentobarbital and perfused transcardially with a mixture of 1% paraformaldehyde and 2% glutaraldehyde in 0.1 M phosphate buffer at pH 7.4. A block of tissue containing the lateral geniculate nucleus was then stereotaxically blocked, removed from the brain, placed in 0.1 M phosphate buffer, and stored in a refrigerator for up to 18 h. The block of tissue was cut on a vibratome in the coronal plane at 100  $\mu$ m, and the sections were reacted with either diaminobenzidine (DAB) (30) or the cobalt intensification modification of the DAB reaction (1).

Recovered neurons were traced at a magnification of 1,000 by using a drawing tube attached to a microscope equipped with a 100 $\times$  oil-immersion objective (NA 1.32). A Kodak Wratten 48A filter was used to increase contrast and improve resolution because of its narrow-band, short-wavelength transmission (cf. Refs. 14, 15). Many sections were subsequently counterstained with cresyl violet to allow comparison of the soma sizes of our injected cells with the soma sizes of the neurons in the surrounding tissue. The somata of the surrounding cells in the parvocellular C-laminae (i.e., cells below the upper half of lamina C, where many Y-cells are located) were traced with the same optics as used for our intracellularly injected neurons. Only cells with visible nucleoli were included. The cross-sectional areas of these somata were measured from the tracings with a planimeter.

In six experiments we injected 0.1 mCi of tritiated proline into the vitreous of one eye for transport by ganglion cell axons to the lateral geniculate nucleus. After the injected W-cells were traced, the geniculate tissue was processed for autoradiography according to the procedure of Cowan et al. (6). Exposure time adequate to demonstrate the individual parvocellular C-laminae was 8–16 wk. Since the individual parvocellular C-laminae are difficult to distinguish in Nissl-stained material, these injections allowed us to assess reliably the laminar relationships of the injected W-cells (22).

### *Statistics*

Unless otherwise stated, all statistical comparisons noted in RESULTS are based on the Mann-Whitney *U* test, and all probability values are one tailed.

## RESULTS

We considered a geniculate neuron recorded in the C-laminae to be a W-cell if, compared to X- and Y-cells, it exhibited a long response latency to electrical stimulation of the optic chiasm and responded poorly and sluggishly to visual stimuli (5, 49,

53). As noted in DISCUSSION, it is not yet clear whether these geniculate W-cells form a single class (analogous to the X- or Y-cell class) or whether they represent several distinct classes. Nonetheless, we shall refer to these as W-cells until we have a more complete classification that requires different terminology.

By these criteria, each of the 60 cells recorded ventral to a tier of Y-cells at the top of lamina C was identified as a W-cell. No X-cell was identified among our population of C-laminae neurons. Of the 60 W-cells, 20 were successfully impaled, injected with HRP, and analyzed morphologically. Most of our description below is limited to these 20 W-cells; 18 had apparently complete HRP staining of somata and dendrites but 2 were incompletely filled beyond the somata and proximal dendrites. Thus, morphological data relevant to dendrites were obtained from 18 W-cells, but all 20 of these neurons provided data relevant to somata. Of the 18 completely stained W-cells, 16 exhibited well-filled axons that could be traced for many sections into the A-laminae, and 9 were followed beyond the lateral geniculate nucleus into the optic radiation. Most of these cells can thus be considered relay cells (cf. Ref. 14).

#### *Response properties of W-cells*

Responsiveness to visual stimuli of the 20 morphologically identified W-cells ranged from unresponsive (5 neurons), through poorly and inconsistently responsive such that receptive-field borders could not be reliably mapped (6 neurons), to sufficiently responsive to map borders (9 neurons). The expected receptive-field location of each unresponsive neuron was approximately known because each was recorded immediately after encountering responsive cells (see METHODS). We cannot rule out the unlikely possibility that the retinotopic map in the C-laminae is grossly discontinuous such that some cells have receptive fields greatly displaced from the majority. Perhaps our "unresponsive" cells were indeed responsive but had such displaced fields that they were missed. Also, it is possible that with more extensive response averaging than we used, visual responses would have been evident for all of these cells. However, because poorly responsive cells are easily missed electrophysiolog-

ically, particularly if they exhibit low spontaneous activity, they may be considerably underrepresented in our sample. The sample, in any case, appears to represent a continuum of responsiveness, and we therefore included unresponsive cells as W-cells. This tentative classification is supported by morphological data presented below.

Response properties of the 20 morphologically identified W-cells in no way seem to represent a biased sample of W-cells recorded in the C-laminae. For instance, Fig. 1 shows how the 20 filled W-cells compare against all recorded W-cells in terms of optic chiasm latency (Fig. 1A) and receptive-field center

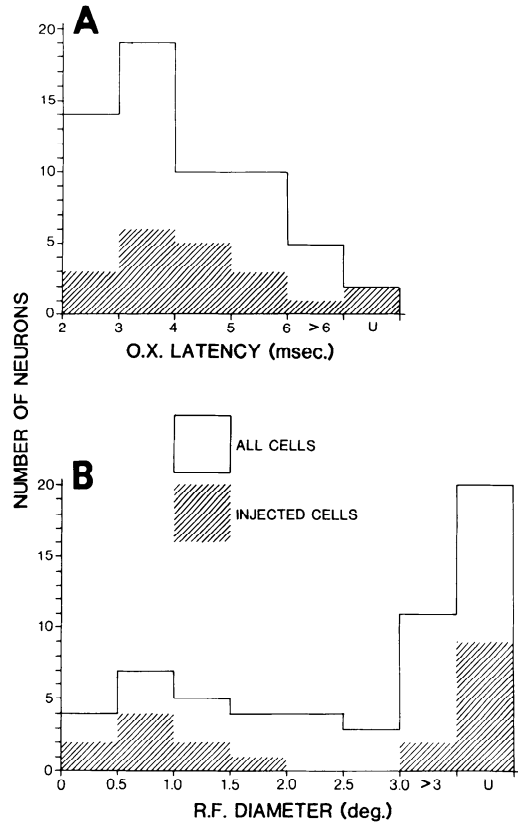


FIG. 1. Comparison of all 60 geniculate W-cells recorded in C-laminae with the subpopulation of 20 that were injected with HRP and recovered for morphological analysis. No differences are evident between the entire population and the subpopulation injected with HRP. *A*: frequency histogram of latencies to electrical stimulation of the optic chiasm. U refers to cells unresponsive to such stimulation. *B*: frequency histogram of receptive-field diameters. U refers to cells too poorly responsive to map their receptive fields.

diameter (Fig. 1*B*). Only 8 of the 20 W-cells responded sufficiently well to counterphased, sine-wave gratings to be assessed in terms of spatial and temporal summation properties. Six of these exhibited linear summation and two were nonlinear (cf. Ref. 49). For each of the W-cells studied that responded to the gratings, including W-cells not identified morphologically, the best response was always elicited to gratings of low spatial and temporal frequency (i.e., <0.5 cycle/deg and <2 Hz).

### Morphology of W-cells

The geniculate W-cells in the C-laminae are rather heterogeneous in morphology. However, they are all morphologically distinct from geniculate X- and Y-cells as described by Friedlander et al. (14), and these

W-cells do share certain structural features with one another. In general, their somata are medium in size and their dendrites, which are rather thin, are oriented parallel to the lamination. In this regard they resemble the class 4 cell described by Guillery (19) from Golgi-impregnated material. Figure 2 presents drawings of the somata and dendrites of four typical C-laminae W-cells, and Table 1 summarizes a number of physiological and morphological parameters for the W-cells illustrated in this report.

**SOMATA.** The soma size distributions of geniculate W-cells are shown in Fig. 3 in comparison to soma sizes of geniculate X- and Y-cells. The sizes of W-cell somata (mean cross-sectional area of  $195 \mu\text{m}^2$ ) and X-cell somata (mean of  $219 \mu\text{m}^2$ ) are comparable ( $P > 0.1$ ), and both are smaller than Y-cell

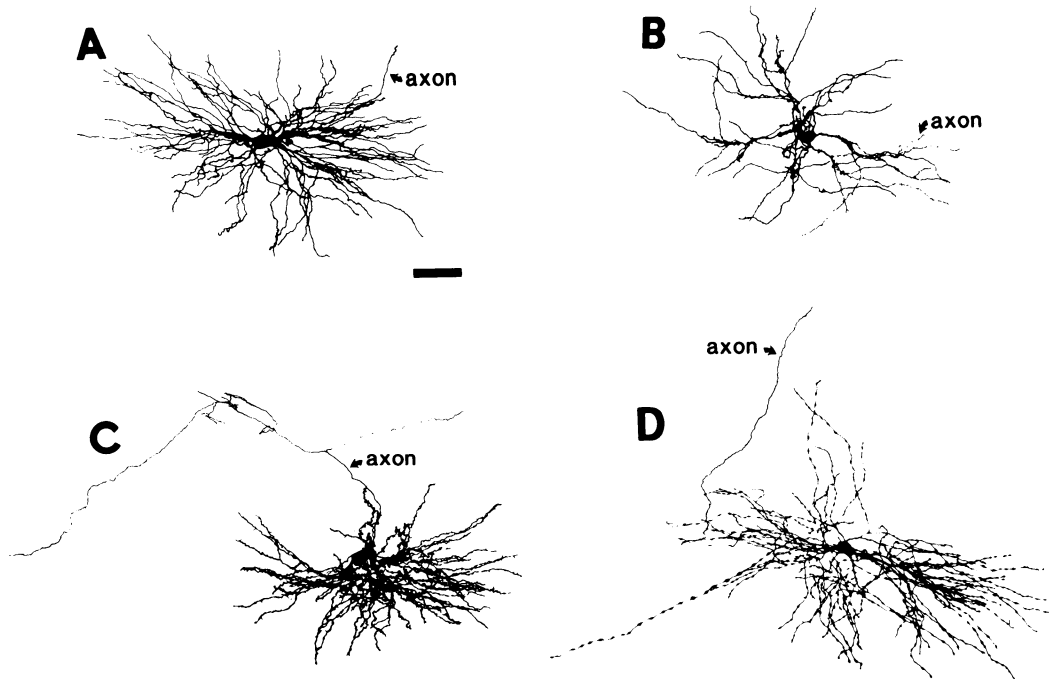


FIG. 2. Camera lucida drawings reconstructed from serial,  $100\text{-}\mu\text{m}$ -thick sections of four representative geniculate W-cells that illustrate the range of dendritic features seen in our sample. The scale applies to each cell; it is  $50 \mu\text{m}$  and is oriented parallel to the geniculate laminae. *A*: W-cell with varicose dendrites (also illustrated in Fig. 5*F*). Dendrites show fairly regular variations in thickness beyond the primary branch point. *B*: W-cell with grapelike clusters appended at or near dendritic branch points (also illustrated in Figs. 5*C* and 17*A*). *C*: W-cell with complex, stalked appendages all along the dendrites (also illustrated in Fig. 5*E, G, H*). The axon branches dorsal to the soma. The leftward branch gives rise to a dense intrageniculate collateral arbor that is further illustrated in Figs. 14*F* and 15*D-G*. *D*: W-cell with beaded appendages (also illustrated in Fig. 5*A, B, D*; another example is shown in Fig. 11*E, F*). Dendrites beyond the primary branch point consist of swollen regions connected by very thin segments. Varicose and beaded dendrites may differ only in the degree of the variation in thickness (see text).

TABLE 1. *Parameters of W-cells further illustrated in various figures*

Cell Illustration, Fig.	Optic Chiasm Latency, ms	Receptive-Field Center Size, deg	Center Type	Receptive-Field Eccentricity, deg	Soma Size, $\mu\text{m}^2$	Dendritic Type
2A; 5F; 14D; E; 18	4.5	1.5	On	3.5	253	Varicose
12	2.5	1.0	On	4.5	164	Varicose
13	5.5	*	On	1.0	237	Varicose
2B; 5C; 17A	4.0	0.5	On	3.0	156	Appendages
10B	2.5	*	*	6.5	304	Beaded
10A; 11	5.5	*	Off	21	233	Beaded
10D	4.8	1	Off	12.5	137	Beaded
2D; 5A; B, D; 10C	4.0	5	Off	5	198	Beaded
2C; 5E, G, H; 14F; 15D-G	4.0	0.5	On	1.5	376	Appendages
14A, C; 15A-C	5.5	*	*	7	253	Varicose

\* Responses too inconsistent or sluggish to evaluate.

somata (mean of  $493 \mu\text{m}^2$ ;  $P < 0.001$  for either comparison). Despite their similarity in size, X- and W-cell somata can be distinguished from each other on the basis of shape: X-cell somata are conspicuously elongated along an axis perpendicular to the lamination, whereas W-cell somata are elongated along an axis parallel to the lamination.

We argue above that our morphologically identified sample of W-cells is fairly representative of those that can be recorded in the C-laminae (e.g., Fig. 1). Figure 4 shows that this sample is also fairly representative of what is actually present in the C-laminae

based on Nissl-stained material. The upper histogram shows the size distribution of HRP-filled somata, and the lower histogram shows the size distribution of 237 other cells from the same, Nissl-stained sections. To omit Y-cells from these measures, the lower histogram excludes the dorsal, magnocellular tier of lamina C. Although the HRP-filled somata appear to be slightly larger, the neuronal numbers are small and there is no statistical difference between the HRP-filled and Nissl-stained samples ( $P > 0.1$ ). We therefore conclude that our electrodes were not strongly biased in favor of larger somata (see also DISCUSSION). While we cannot rule out other forms of electrode sampling bias (based on

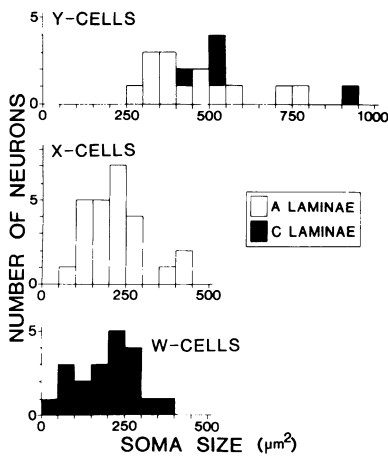


FIG. 3. Some size histograms of geniculate W-, X-, and Y-cells that were filled with HRP. The X- and Y-cell data were redrawn from Friedlander et al. (14) and A- and C-laminae neurons are separately indicated. W- and X-cell somata are comparable in size and both are smaller, on average, than are Y-cell somata.

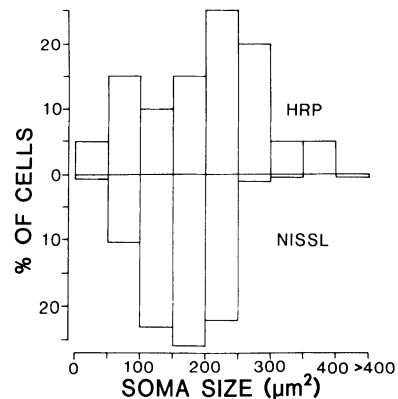


FIG. 4. Comparison of soma sizes of 20 geniculate W-cells injected with HRP (upper) and those of 237 surrounding Nissl-stained neurons (lower) from the same sections in the parvocellular C-laminae. No significant difference is evident between these distributions.

dendritic configurations, neuronal activity, etc.), our data probably contain a fairly representative sample of C-laminae neurons. Friedlander et al. (14) arrived at a similar conclusion for their intracellularly injected X- and Y-cells in the A-laminae.

**DENDRITES. Individual dendrites.** Morphological features of neurons within the W-cell class are remarkably heterogeneous. Figures 2 and 5 provide examples of this heterogeneity. The cell in Figs. 2*A* and 5*F* has relatively smooth dendrites that are nearly free

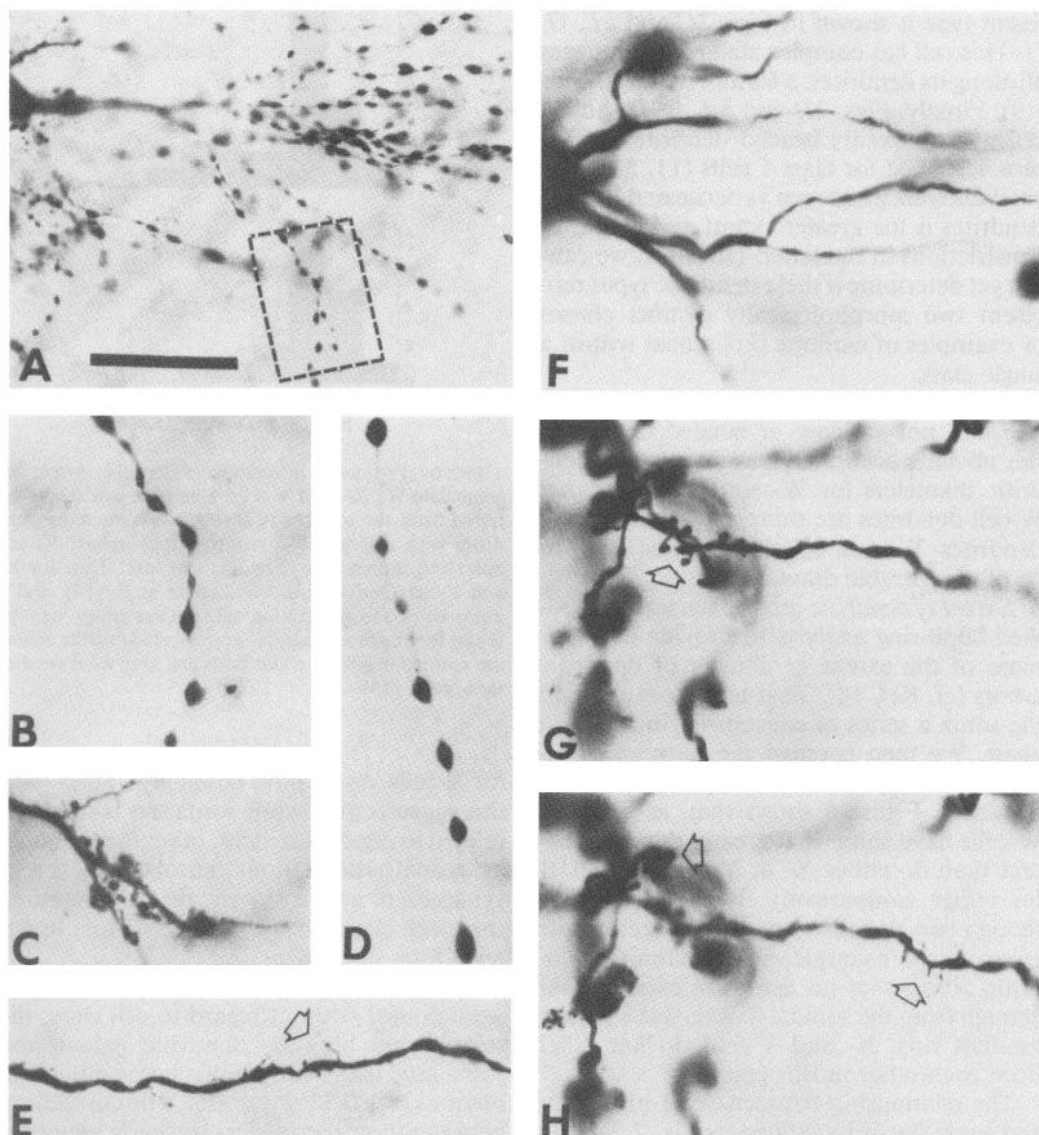


FIG. 5. Photomicrographs of representative dendrites from geniculate W-cells. The scale in *A* represents 50  $\mu\text{m}$  for *A* and *F* and 20  $\mu\text{m}$  for *B-E*, *G*, and *H*. *A*: lower power view of W-cell with beaded dendrites. The soma is at the upper left, and the dashed lines enclose the view shown in *B*. A complete reconstruction of the cell is shown in Fig. 2*D*. *B*: higher power view of beaded segment of dendrite from cell in *A*. *C*: grapelike clusters appended near branch point of dendrites from cell shown in Fig. 2*B*. *D*: another view of beaded dendritic segment from cell shown in *A*. *E*: portion of dendrite from cell shown in Fig. 2*D* with complex, stalked appendages. The arrow points to one of these appendages. *F*: portion of cell drawn in Fig. 2*A* with varicose dendrites beyond the primary branch point. *G*, *H*: two focal planes of same field of view of cell drawn in Fig. 2*D*. Arrows indicate complex, stalked structures appended to the dendrites. A different dendritic segment of this cell is shown in *E*.

of any appendages, one of the characteristics of class 1 cells (19); beyond the primary branch point, these dendrites generally become varicose. Figures 2B and 5C represent a cell that has many grapelike clusters of appendages at dendritic branch points, one of the features of class 2 cells (19). Yet a different type is shown in Figs. 2C and 5E, G, H. This cell has complex stalked appendages all along its dendrites, a feature of class 3 cells (19). Finally, Figs. 2D and 5A, B, D show a cell with markedly beaded dendrites, a feature described for class 5 cells (11, 51). The chief difference between varicose and beaded dendrites is the greater extent and length of constrictions in the latter. However, we cannot yet determine if these dendritic types represent two morphologically distinct classes or examples of extreme differences within a single class.

Only rare W-cell dendrites are appendage free and not varicose or beaded. Although this obviates accurate measurements of dendritic diameters for W-cells, it is clear that W-cell dendrites are thinner than are Y-cell dendrites. W- and X-cell dendrites seem to be of comparable diameter.

*Extent of dendritic arbors.* We used a modified Sholl-ring analysis to provide one estimate of the extent or density of dendritic arbors (cf. Ref. 14). That is, we centered on the soma a series of concentric rings 50  $\mu\text{m}$  apart. We then counted the number of intersections made by these rings and the cell's dendrites. Figure 6 shows that, as a group, W-cells have somewhat greater dendritic extent than do either X- or Y-cells ( $P < 0.01$  for either comparison). This is true even though two W-cells were the only geniculate neurons in our sample with such limited dendritic arbors that no dendrites extended far enough from the somata to intersect even the smallest ring. X- and Y-cells do not differ from each other in this regard ( $P > 0.1$ ).

The relationship between dendritic extent and soma size is illustrated by Fig. 7. Within each neuron class, these variables are highly and significantly correlated (W-cells:  $r = 0.78$ ,  $P < 0.001$ ; X-cells:  $r = 0.82$ ,  $P < 0.001$ ; Y-cells:  $r = 0.83$ ,  $P < 0.001$ ). However, the precise relationship differs among the classes. Increases in soma size are associated with the greatest dendritic increase for W-cells, least for Y-cells, and intermediate

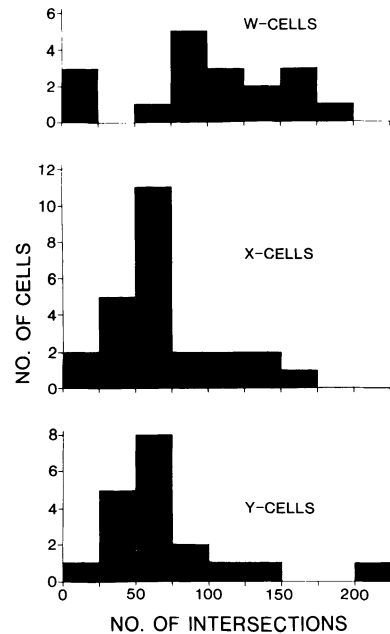


FIG. 6. Frequency histograms of dendritic extent for geniculate W-, X-, and Y-cells. Dendritic extent was inferred from the number of intersections made by dendrites with a series of concentric rings spaced 50  $\mu\text{m}$  apart and centered on the soma (see text). Data for X- and Y-cells derive from Friedlander et al. (14), and a more complete description of this parameter can be found there. On average, X- and Y-cell dendritic arbors are comparable in size and both are somewhat smaller than those of W-cells.

for X-cells. As we have noted previously (14), this suggests that, while soma size is certainly related to dendritic extent, other factors (such as axonal arborizations, number of efferent synapses, or activity levels) that differ among these cell classes must also play a role in determining soma size.

Finally, note that if all the data in Fig. 7 were pooled without regard to cell class, the relationship between dendritic extent and soma size, while still significant, is much less obvious ( $r = 0.33$ ;  $P < 0.01$ ). The correlation between these parameters is clearly better for each of the individual W-, X-, and Y-cell classes than for the entire population of neurons ( $P < 0.001$  on each comparison of correlation coefficients). Whatever the significance of this relationship between somata and dendritic arbors, it is clearer when cells are grouped according to physiological properties.

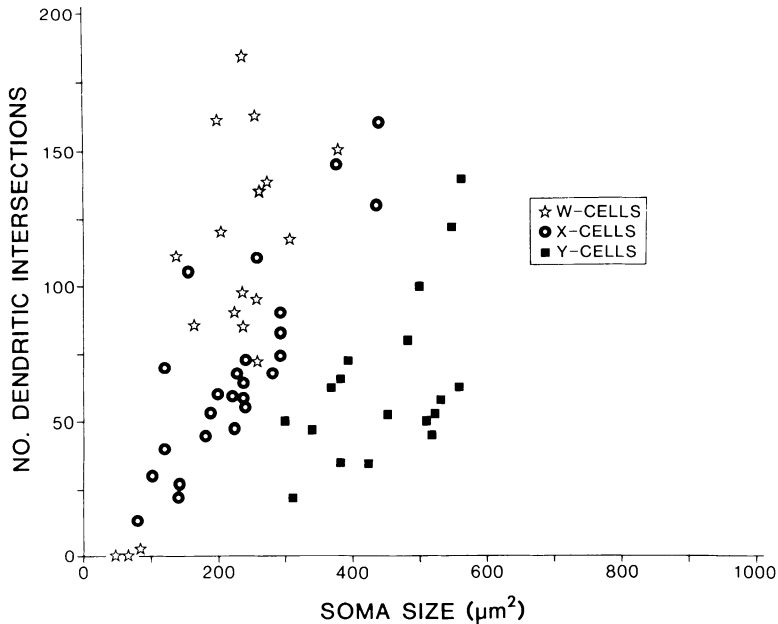


FIG. 7. Relationship between dendritic extent (as measured by the number of dendritic intersections with a series of concentric rings; see text) and soma size for geniculate W-, X-, and Y-cells. The X- and Y-cell data were redrawn from Friedlander et al. (14). Two W-cells are shown with zero dendritic intersections because none of their dendrites extended far enough to reach the ring nearest to the soma's center,  $50 \mu\text{m}$  away. Note that the correlation between dendritic extent and soma size is much better for each of the separate W-, X-, and Y-cell classes than for the entire population of neurons pooled together.

*Shape of dendritic arbors.* As is evident from drawings of HRP-filled W-cells (e.g., Fig. 2), there exists a striking lack of circular symmetry in their dendritic arbors. There is a marked tendency for these dendrites to lie in a plane parallel to the lamination. We investigated this feature more systematically by means of the Sholl-ring analysis described above. The rings were divided into four adjacent quadrants: two perpendicular to the geniculate lamination and two parallel to these laminae. For a given neuron, the quadrants of the Sholl rings were oriented appropriately with respect to the geniculate laminae. Here and below, horizontal refers to an orientation parallel to the geniculate laminae and vertical refers to one perpendicular to these laminae.

Figure 8 plots for each W-cell the number of intersections made between the dendrites and rings, and it shows these values separately for the vertical and horizontal quadrants. For comparison, our earlier published data for geniculate X- and Y-cells (14) are also shown. The line of slope 1 is drawn to

indicate the locus of neurons with circular symmetry. Every W-cell that had dendritic intersections (see above) falls below this line. By contrast, every X-cell falls above the line and every Y-cell but one lies close to the line. This verifies our qualitative observations that W-cells have dendritic arbors that are horizontally elongated, that X-cell dendritic arbors are vertically elongated, and that Y-cell arbors generally exhibit circular symmetry.

Three-dimensional measurements of the dendritic configuration of the HRP-filled neurons were made as follows. Each  $100\text{-}\mu\text{m}$  coronal section was optically divided into 10 equally spaced coronal slices by means of the fine-focus micrometer on a Leitz Orthoplan microscope. Although the sections were less than  $100 \mu\text{m}$  thick after cover slipping, we assumed that any compression was constant throughout the thickness of each section. Thus we were able to obtain information about the anteroposterior axis of these coronal sections with a resolution of approximately  $10 \mu\text{m}$ , and this was combined with the higher resolution information available

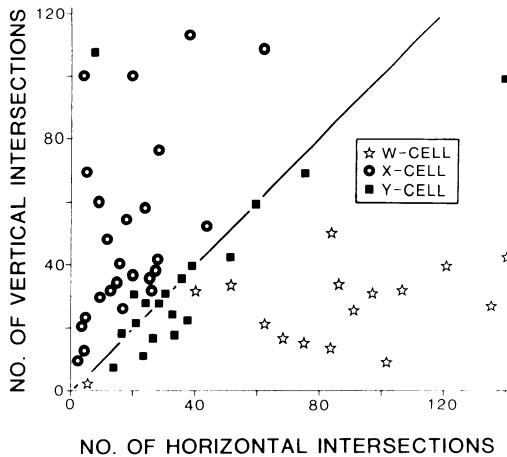


FIG. 8. Vertical versus horizontal extent of dendritic arbors for geniculate W-, X-, and Y-cells. The X- and Y-cell data were described by Friedlander et al. (14). For each neuron, a series of concentric rings spaced at 50- $\mu$ m intervals was centered on the soma and divided into two vertical and two horizontal quadrants with respect to the orientation of the geniculate laminar borders (see text for details). The number of intersections made in the vertical and horizontal quadrants was plotted for each cell. The line of slope 1 is drawn to indicate the locus of points expected for a dendritic arbor with circular symmetry. The two W-cells represented in Fig. 7 with no dendritic intersections are omitted from this illustration. Note that every X-cell falls above the line (thus showing a vertical bias in their dendritic arbors), every W-cell falls below the line (thus showing a horizontal bias in their arbors), and every Y-cell but one falls fairly near the line (thus showing approximate circular symmetry in their arbors).

in the coronal plane to produce a rough three-dimensional reconstruction. These reconstructions indicate that the dendritic arbor of each W-cell roughly approximates a short, right cylinder or disk with its altitude oriented perpendicular to the geniculate laminar borders and its intersection with the plane parallel to these borders roughly being circular (see also Ref. 19). The mean dimensions of these cylinders are an altitude of 260  $\mu$ m (i.e., the vertical extent of dendrites) and a directrix diameter of 410  $\mu$ m (i.e., the horizontal extent). In contrast, X-cell dendritic arbors form right cylinders with the altitudes perpendicular to the geniculate laminar borders, and those of Y-cells are more or less cylindrical (14). For the 10 X- and 10 Y-cells illustrated in Fig. 9, the mean dimensions are an altitude of 310  $\mu$ m plus a directrix di-

ameter of 170  $\mu$ m for the X-cells and a diameter of 360  $\mu$ m for the Y-cells.

*Spatial relationship between dendritic arbors and somata.* Because dendrites represent the cell's major postsynaptic region and because postsynaptic potentials are thought to be electrotonically conducted from these dendrites to the soma and axon hillock, the spatial relationship between the dendritic arbor and soma may prove to be of some importance. To assess these relationships, we used our Sholl-ring analyses to determine the extent of the dendritic arbor (cf. Fig. 6) and the asymmetry of the arbor (cf. Fig. 8) as a function of distance from the soma in four 50- $\mu$ m steps. Figure 9 summarizes some of these relationships for the W-cells of this study as well as 10 X- and 10 Y-cells reanalyzed from the data of Friedlander et al. (14).

Figure 9A summarizes the average extent of the dendritic arbor as a function of distance from the soma for these W-, X-, and Y-cells. The vast majority of the arbor is found within 100  $\mu$ m of the soma for each cell class. The tendency at the 50- $\mu$ m distance for X-cells to concentrate somewhat more of their arbors than do W- or Y-cells is not statistically significant ( $0.1 > P > 0.05$ ). Generally, the three cell classes show a similar distribution of dendritic extent with distance from the soma.

Also, a "symmetry index" was computed for each cell by counting the number of intersections in the horizontal and vertical quadrants and dividing the smaller number by the larger. The maximum value of 1.0 indicates a circularly symmetrical dendritic arbor, and lower values indicate decreasing circular symmetry. Figure 9B summarizes these values of the symmetry index averaged across the W-, X-, or Y-cells as a function of distance from the soma. Each of the W-cell dendritic arbors lacked circular symmetry, with more intersections in the horizontal quadrants, and this was evident for each neuron at every distance measured from the soma. Likewise, each X-cell arbor lacked circular symmetry, with more intersections in the vertical quadrants, and this was seen at each distance measured from every cell. The tendency for this lack of circular symmetry to be less pronounced at 50  $\mu$ m from the soma than further away was significant

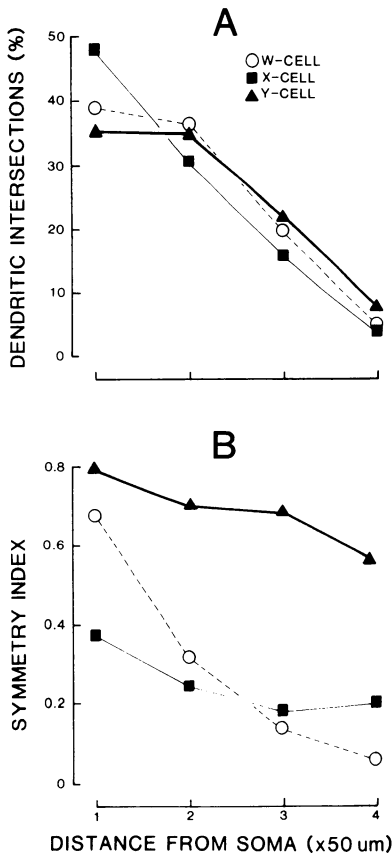


FIG. 9. Geometry of dendritic arbors as a function of distance from the soma for geniculate W-, X-, and Y-cells. Four sampling locations were taken at steps of 50  $\mu\text{m}$  from the soma center by calculating the number of dendritic intersections made with each concentric circle (see text). Data were taken from the 16 W-cells shown in Fig. 8 plus 10 X- and 10 Y-cells randomly chosen for analysis from the data of Friedlander et al. (14). Each point represents an average value for the W-, X-, or Y-cells as indicated. *A*: dendritic extent as a function of distance from the soma center. The total number of dendritic intersections with all four rings was counted, and the percentage with each ring is plotted. All three cell classes exhibit a similar tendency to concentrate their dendritic arbors within 50 or 100  $\mu\text{m}$  of the soma. *B*: symmetry index as a function of distance from the soma. To compute this index, the concentric rings were divided into vertical and horizontal quadrants, as described for Fig. 8. Then, the number of intersections between dendrites and these rings in the less-represented quadrants (i.e., vertical or horizontal) was divided by the number in the other quadrants. Perfect circular symmetry is represented by an index of 1.0, and progressively lower numbers indicate arbors with increasing circular asymmetry. Every X-cell exhibited a vertical bias (i.e., more intersections in the vertical quadrants) at each distance; every W-cell exhibited a horizontal bias at each distance; and Y-cell values were more variable both among cells and among distances within

for W-cells ( $P < 0.001$ ) but not for X-cells ( $0.1 > P > 0.05$ ). At this 50- $\mu\text{m}$  distance, W-cell arbors were more circularly symmetrical than were those of X-cells ( $P < 0.001$ ), but otherwise no differences between W- and X-cells were seen in this measure except for the obvious difference in the major axis (horizontal versus vertical) of the circular asymmetry.

Of the relatively symmetrical Y-cell arbors, six had more dendritic intersections in the horizontal quadrants and four in the vertical quadrants. Also, for several Y-cell arbors, the direction of the circular asymmetry (horizontal versus vertical) changed at different distances from the soma. Y-cells, on average, displayed the same circular symmetry of their dendritic arbors regardless of distance from the soma. Also, except for the 50- $\mu\text{m}$  distance from the soma, where W- and Y-cell arbors are equally symmetrical ( $P > 0.1$ ), Y-cell arbors are more circularly symmetrical at every distance than are those of W- or X-cells ( $P < 0.001$  for each comparison).

*Translaminar dendrites.* It might be suggested that the shape of W-cell dendritic trees is dictated by their location within the extremely thin parvocellular C-laminae. That is, if W-cell dendrites must for some reason occupy only a single lamina, then their dendrites are likely to become oriented parallel to the laminar borders. Unfortunately, individual C-laminae cannot be visualized in standard Nissl preparations but instead require a means of delineating retinal input from each eye.

In order to address the question of location of dendritic trees with respect to these laminar borders, we injected the vitreous of one eye in each of six cats with tritiated proline and subsequently processed the brain for autoradiography. This was done approximately 1 wk before recording and intracellular HRP injection of W-cells. Because autoradiography shows laminar borders only for the few micrometers of the 100- $\mu\text{m}$ -thick section subjacent to the photographic emulsion, we considered the possibility that these borders

a cell. The W-cell dendritic arbors become increasingly asymmetrical with increasing distance from the soma, but X- and Y-cell arbors exhibit little change with distance.

shifted deeper in the sections where many HRP-filled processes were located. This was ruled out as a serious artifact in interpreting the laminar location of W-cell processes for two reasons. First, the laminar borders were ascertained for a series of adjacent sections, and their locations could be interpolated within the sections. Shifts of these borders in the neighborhood of filled W-cells were judged to be relatively gradual. Second, each of the dendritic arbors of these W-cells traversed several adjacent sections, and some processes of each could always be located sufficiently close to the emulsion to verify the main conclusion that some translaminar dendrites were present for each of these cells.

Eight of our recovered W-cells were obtained from these autoradiographic experiments, and thus we can confidently locate these neurons with respect to the individual

C-laminae. The soma of each was located in a lamina appropriate for physiological ocular dominance (e.g., lamina C1 for an ipsilateral eye's receptive field and lamina C2 for the contralateral eye's receptive field). Furthermore, each had at least some dendrites that crossed into a neighboring lamina. Figures 10 and 11 illustrate examples of this. Note that the cell shown in Fig. 10A has a soma and many dendrites in lamina C1, but nearly half of its dendritic tree ramifies in lamina C2. Also, the cell illustrated in Fig. 10C has a soma in lamina C2 and some dendrites that cross several laminar borders to terminate in lamina C. While the pattern of lamination may play some role in the orientation of W-cell dendrites, it seems safe to conclude that these dendrites are not powerfully constrained by laminar boundaries.

Consistent with this conclusion is the ob-

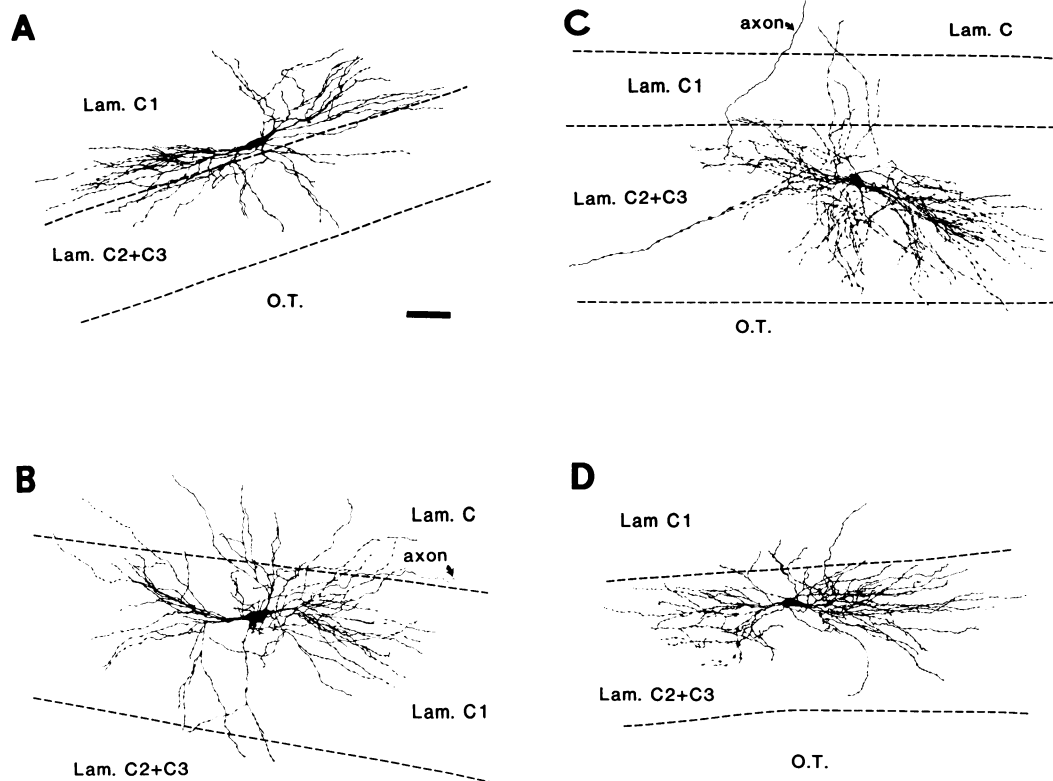


FIG. 10. Camera lucida drawings of four geniculate W-cells showing relationships between dendritic arbors and individual C-laminae. These laminae were revealed by autoradiography following intraocular injections of tritiated proline. Because the ipsilateral eye was injected in each case, we could not distinguish lamina C2 from lamina C3 (22). The scale is  $50\ \mu\text{m}$  and applies to all cells. For each cell, a significant fraction of dendrites pass into adjacent laminae. The cell shown in C even has several dendrites that pass from lamina C2 into lamina C1 and then span all of lamina C1 to reach lamina C.

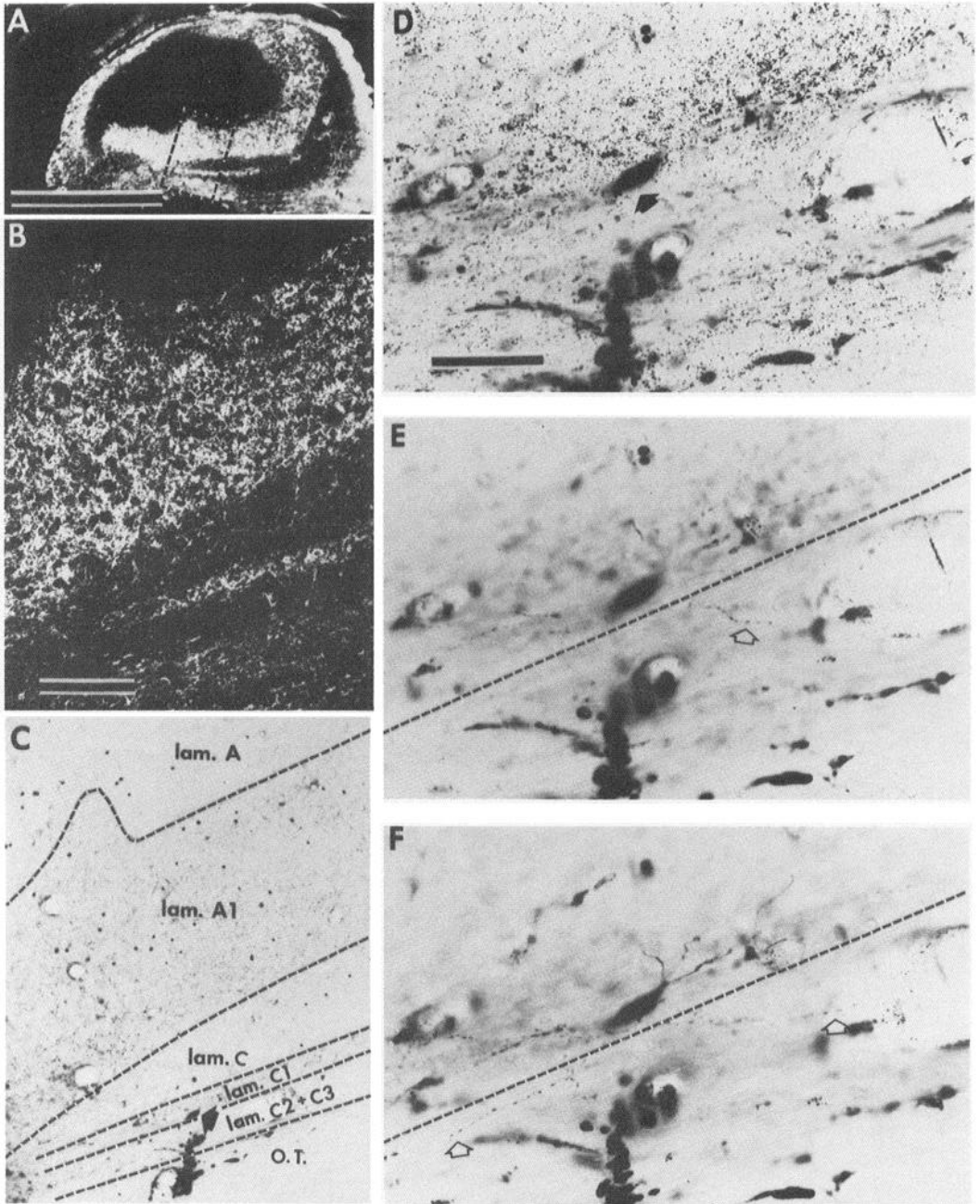


FIG. 11. Photomicrographs to illustrate relationship between dendritic arbors and geniculate laminae for W-cell shown in Fig. 10A. *A*: low-power dark-field view of the left lateral geniculate nucleus. The left eye was injected with tritiated proline, and the resultant autoradiography labels laminae A1 and C1. The box outlines the view in *B* and *C*. The scale is 2 mm. *B*: higher power dark-field view of region outlined in *A*. The scale is 200  $\mu$ m and applies as well to *C*. *C*: bright-field view of same area shown in *B*, with laminar borders as indicated. The solid arrow points to the soma of the W-cell near the ventral border of lamina C1. *D-F*: bright-field views of three focal planes of same area showing the soma and some dendrites. The scale in *D* is 50  $\mu$ m and applies as well to *E* and *F*. In *D*, the focus is on the emulsion, and the soma is indicated by a solid arrow. In *E* and *F*, where the focus is on the soma and dendrites, the border between laminae C1 and C2 is indicated by a dashed line. Notice the fine, beaded dendrites (open arrows) that can be followed into lamina C2.

servation that several of our W-cells near the bottom of the C-laminae have some dendrites that extend ventrally well into the optic tract (Fig. 12; see also Fig. 18). Indeed, one neuron identified physiologically as a W-cell was located entirely in what appears to be optic tract (Fig. 13). That is, it is located ventral to the C-laminae, but its morphology (including horizontally oriented dendrites) is similar to that of other W-cells in this study. A close inspection of Nissl-stained material reveals a few scattered neurons in the optic tract just ventral to the C-laminae, a point previously noted by Guillery and Scott (21). Like the neuron we injected with HRP, these may all be W-cells that represent an irregular extension of the C-laminae or cells that failed to migrate completely to appropriate laminae. If so and if they also have horizontally oriented dendrites, then lamination can hardly play a dominant role in the asymmetry of W-cell dendritic trees.

**W-CELL AXONS.** Of the 18 well-stained W-cells, 16 exhibited axons that could be traced for a considerable distance through the lateral geniculate nucleus and 9 were followed into the optic radiation. The course of these W-cell axons, like those of X- and Y-cell axons, is often quite circuitous and unpredictable. A common trajectory is one that ascends to the border between laminae C and A1, follows this interlaminar zone to the border between the laminated part of the nucleus and the medial interlaminar nucleus, ascends in the fiber zone separating these geniculate subdivisions until the perigeniculate nucleus is reached above lamina A, travels for a variable distance in the perigeniculate nucleus laterally and parallel to lamina A, and finally ascends into the optic radiation (see also below).

As is the case for X- and Y-cells (14), many W-cell axons issue collaterals in the perigeniculate nucleus just dorsal to lamina A. Of

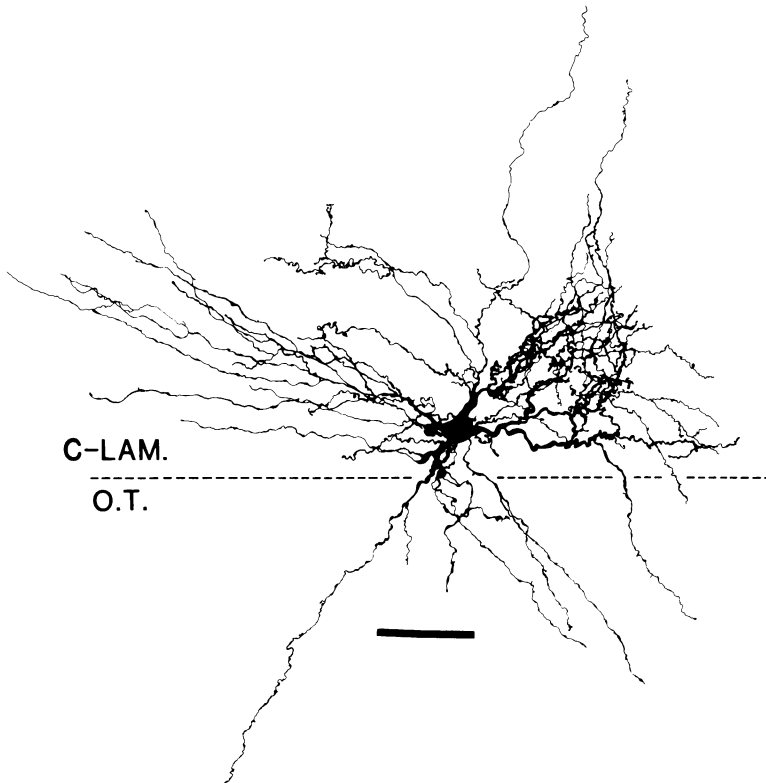


FIG. 12. Camera lucida drawing of a W-cell located near the ventral border (dashed line) of the C-laminae (C-LAM.) with dendrites extending well into the optic tract (O.T.). See also Fig. 18. The scale is 50  $\mu$ m.

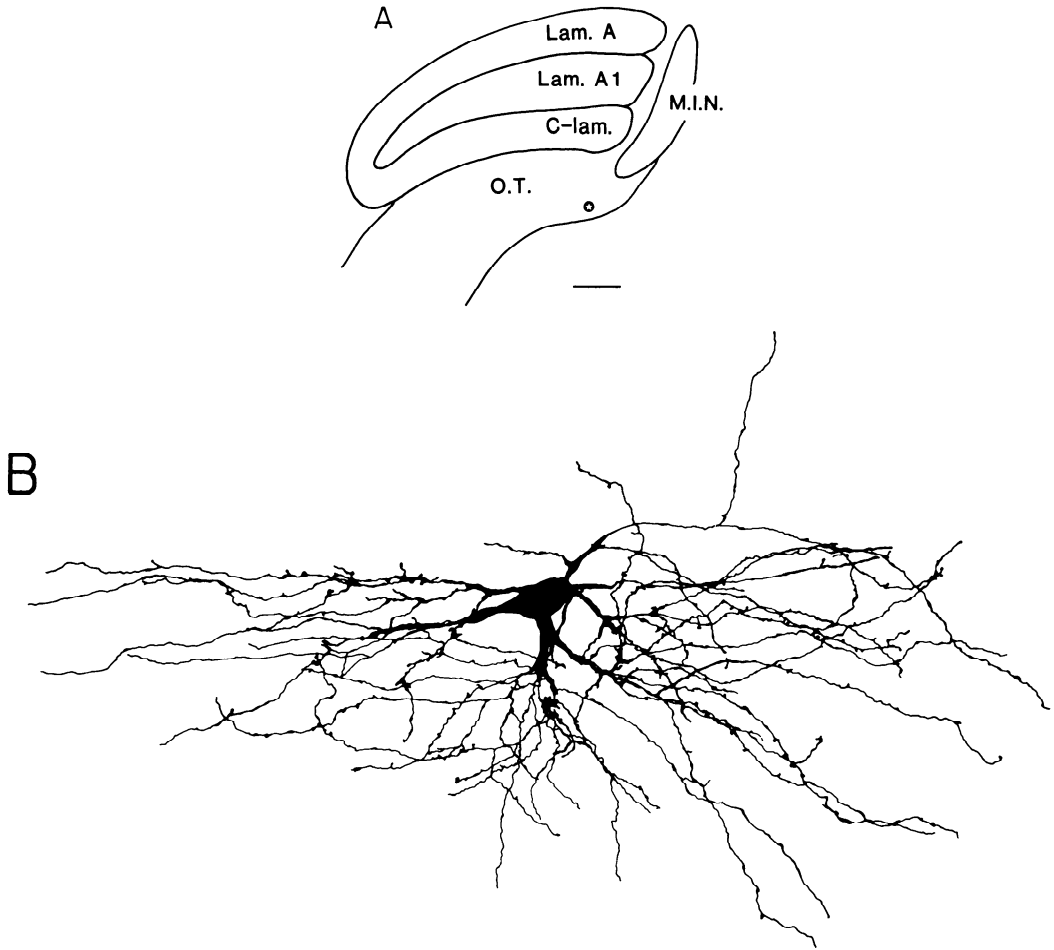


FIG. 13. W-cell located in the optic tract. The scale is  $500\ \mu\text{m}$  for *A* and  $50\ \mu\text{m}$  for *B*. *A*: low-power drawing of coronal section through the lateral geniculate nucleus to illustrate location of the soma (at the star) in the optic tract (O.T.). The main laminae plus the medial interlamina nucleus (M.I.N.) are shown for reference. *B*: camera lucida drawing of the cell.

nine axons traced through this nucleus, seven issued collaterals. Also, of the 16 axons traced for a distance within the lateral geniculate nucleus, 2 issued intrageniculate collaterals. Figure 14 illustrates axon collaterals from three W-cells. One of the cells emitted a perigeniculate collateral (Fig. 14*A, B*), one emitted both types of collateral (Fig. 14*C-E*), and one cell (also illustrated in Fig. 2*C*) issued only an intrageniculate collateral (Fig. 14*F*). Figure 15 shows photomicrographs of the intrageniculate collaterals shown in Fig. 14*C, F*.

Both the perigeniculate and intrageniculate collaterals of W-cells are typified by ex-

trremely fine axon branches that have boutons en passant and terminaux. The fine branches are so thin they can barely be resolved by the light microscope, and often they cannot be followed without gaps that are interpreted as regions in which the collateral is too fine to be detected with the light microscope. It is thus possible that more of these collaterals exist that were not detected by our methods.

Finally, the parent axons of W-cells are quite thin compared to those of X- and Y-cells (see Fig. 16). The axon diameters shown in Fig. 16 were measured to the nearest  $0.5\ \mu\text{m}$ , and each value represents the mean of

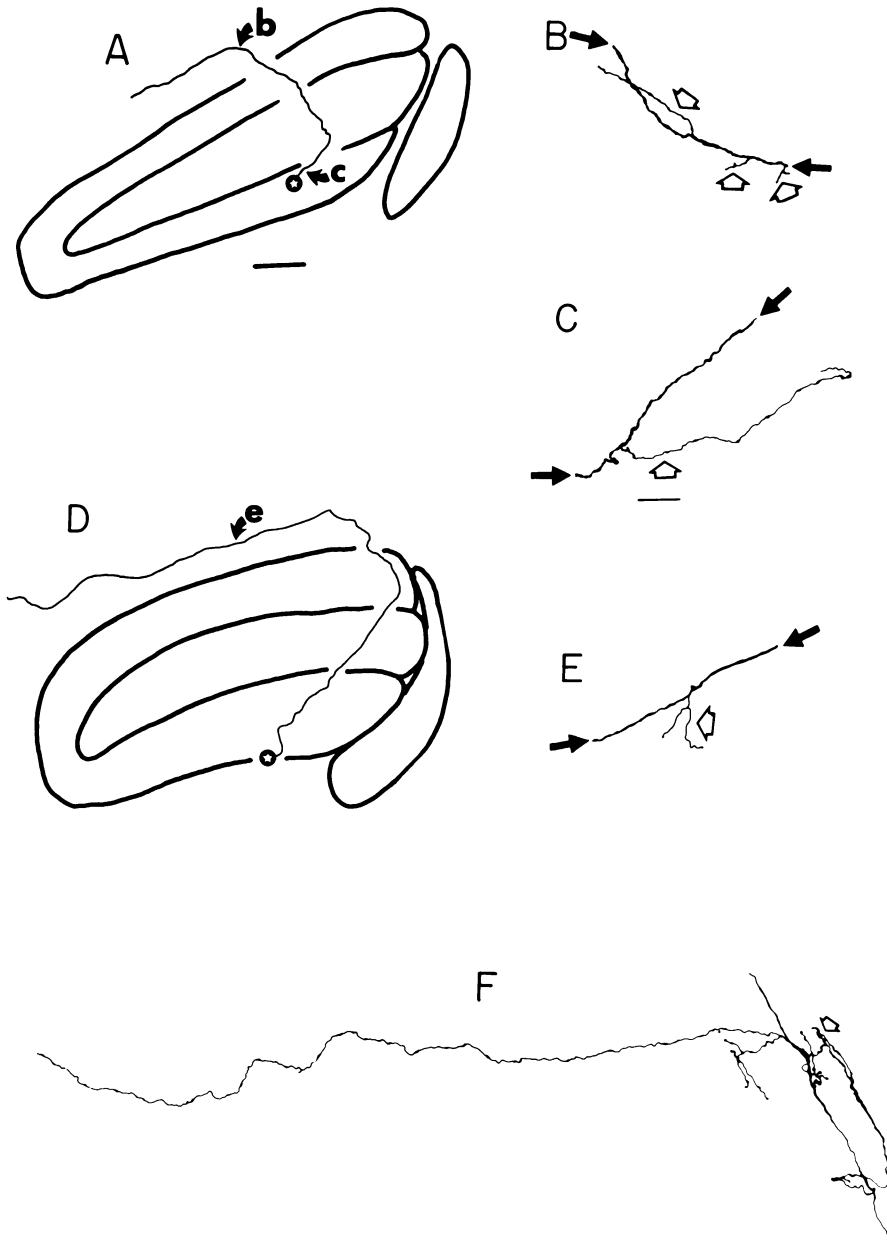


FIG. 14. Axon collaterals of geniculate W-cells. *A*: low-power drawing of coronal section through the lateral geniculate nucleus to show the location of a W-cell soma (star) and the course of its axon. Arrow *b* indicates the location of axon collaterals in the perigeniculate nucleus just dorsal to lamina A, and arrow *c* indicates the location of axon collaterals within C-laminae. The scale is  $500\ \mu\text{m}$  and applies as well to *D*. For identification of laminae and medial interlaminar nucleus in *A* and *D*, refer to Fig. 13*A*. *B*, *C*: details of axon collaterals (open arrows) indicated, respectively, by arrows *b* and *c* in *A*. The main axonal trunk is indicated by the solid arrows. The intrageniculate collateral in *C* is further illustrated in Fig. 15*A-C*. The scale in *C* is  $20\ \mu\text{m}$  and applies as well to *B*, *E*, *F*. *D*: low-power drawing of coronal section through the lateral geniculate nucleus to show the location of a W-cell soma (star), the course of its axon, and the location of perigeniculate collaterals of the axon (*e*). *E*: details of the perigeniculate collateral (open arrow) represented in *D*. The main axonal trunk is indicated by the solid arrows. *F*: details of intrageniculate axonal collateral shown for the W-cell illustrated in Fig. 2*C* and photomicrographs of it are shown in Fig. 15*D-G*. For reference, the open arrow points to the clump of boutons shown in Fig. 15*G*.

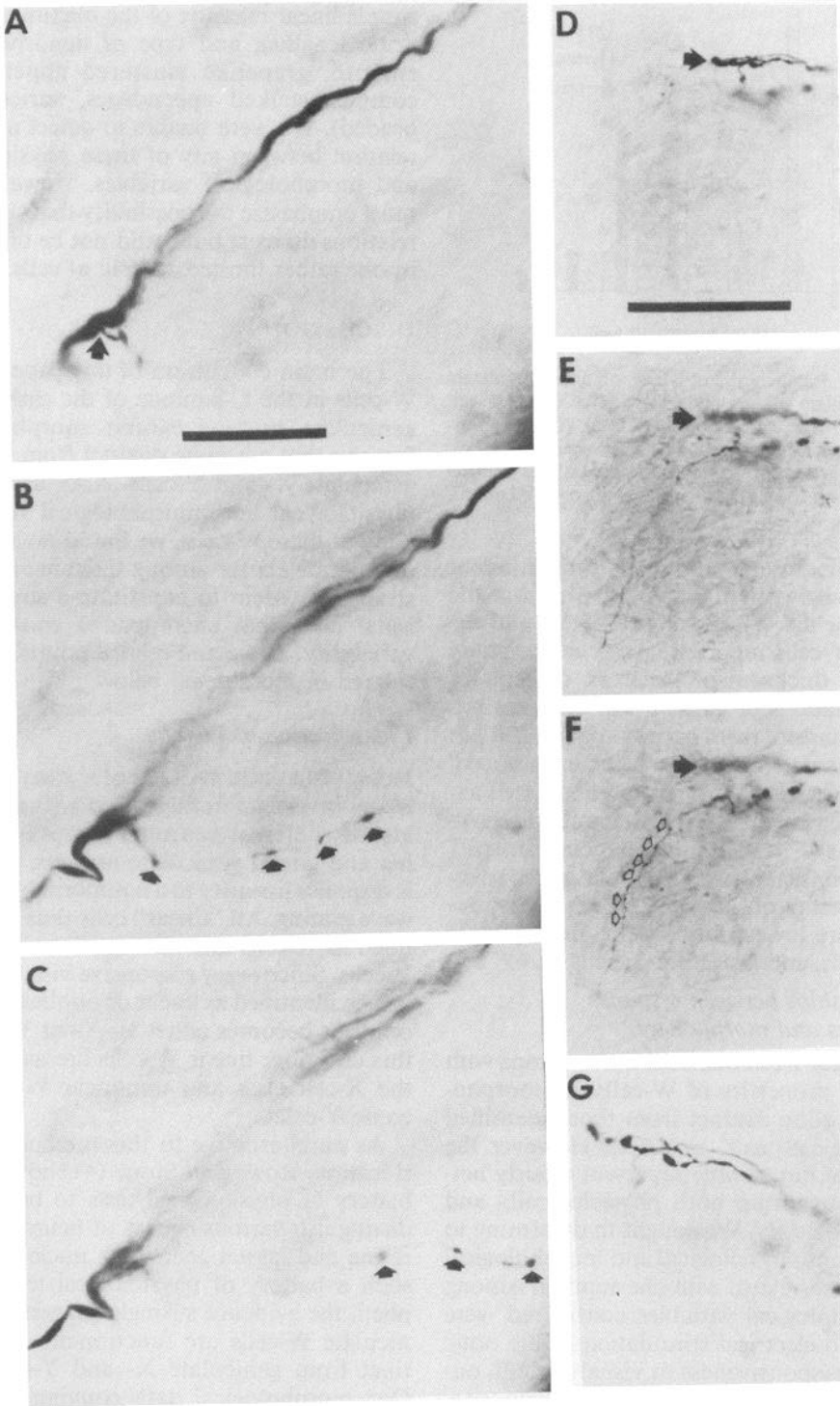


FIG. 15. Photomicrographs of intrageniculate axon collaterals from W-cells. *A-C*: three different focal planes of same view of collateral drawn in Fig. 14*C*. The arrow in *A* shows the branch point between the main trunk of the axon (mostly in focus) and the collateral (mostly out of focus). Arrows in *B* and *C* point to boutons along the collateral. The scale in *A* is 20  $\mu\text{m}$ . *D-F*: three different focal planes of same view of collateral drawn in Fig. 14*F* from W-cell shown in Fig. 2*C*. The open arrows point to boutons along one collateral branch, and the filled arrows depict a bouton cluster on a different branch. The scale in *D* is 50  $\mu\text{m}$ . *G*: higher power view of bouton cluster indicated by filled arrows in *D-F*. The scale in *D* represents 20  $\mu\text{m}$  for *G*.

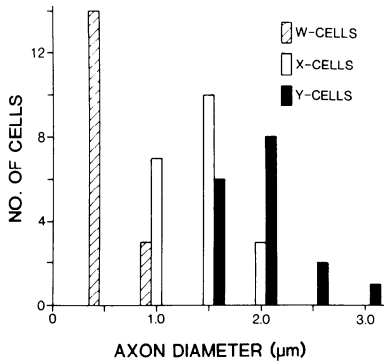


FIG. 16. Frequency histogram of axon diameters from geniculate W-, X-, and Y-cells. The X- and Y-cell data are redrawn from Friedlander et al. (14). Axon diameters have been measured to the nearest 0.5  $\mu\text{m}$ . Despite some overlap, W-cell axons are thinner than X-cell axons, which in turn are thinner than Y-cell axons.

several measurements taken from different locations between 100 and 200  $\mu\text{m}$  from the soma. For the W-cells reported here and the X- and Y-cells reported in our earlier study (14), the thickness of the axon (except for local variations or varicosities) becomes relatively constant from approximately 100  $\mu\text{m}$  from the soma for as long as it can be traced. W-cell axons are thinner than are X-cell axons, which in turn are thinner than are Y-cell axons ( $P < 0.001$  for each comparison). This is consistent with the relative conduction velocities of these cell classes. These velocities are lowest for W-cells, intermediate for X-cells, and fastest for Y-cells (5, 49, 53).

#### *Relationships between response properties and morphology*

It is clear from our data that neurons with response properties of W-cells are morphologically quite distinct from those identified physiologically as X- or Y-cells. However, the W-cells of our sample represent a fairly heterogeneous group both physiologically and morphologically. We sought to determine to what extent physiological and morphological variables correlated with one another. Among the physiological variables considered were latency to electrical stimulation of the optic chiasm, responsiveness to visual stimuli, on- or off-center response, receptive-field size, and linearity of spatial and temporal summation to visual stimuli. Morphological variables included soma size, dendritic extent (based either on our Sholl-ring analysis or a

simple linear measure of the maximum dendritic lengths), and type of dendrites (i.e., smooth, grapelike clustered appendages, complex stalked appendages, varicose, or beaded). We were unable to detect any correlation between any of these physiological and morphological variables. However, we must emphasize the possibility that such correlations do exist but could not be discerned in our rather limited sample of cells.

## DISCUSSION

The main conclusion of this paper is that W-cells in the C-laminae of the cat's lateral geniculate nucleus exhibit morphological features that are quite distinct from those of geniculate X- and Y-cells. Also, despite the physiological and morphological heterogeneity of these W-cells, we found no evidence of separate classes among these neurons. Instead, they seem to constitute a single neuronal class that encompasses considerable variability. These and related points are considered in more detail below.

### *Classification of W-cells*

ARE W-CELLS DISTINCT FROM X- AND Y-CELLS? Many investigators have used a single test to identify different neuronal classes in the retina and lateral geniculate nucleus. This test is response linearity to a counterphased, sine-wave grating. All "linear" cells thus are identified as X-cells and all "nonlinear" cells as Y-cells. Since every responsive visual neuron can be identified as linear or nonlinear, every cell thus becomes either an X- or Y-cell. By this criterion, linear W-cells are assigned to the X-cell class and nonlinear W-cells become Y-cells.

As an alternative to this method of classification, Rowe and Stone (41) advocated a battery of physiological tests to be used to distinguish various classes of neurons in the retina and lateral geniculate nucleus. When such a battery of physiological tests is applied, the evidence strongly suggests that geniculate W-cells are functionally quite distinct from geniculate X- and Y-cells (49). Our morphological data convincingly support this conclusion because it is clear that W-cells represent neurons with structural features quite distinct from and not continuous with those of X- or Y-cells (see Figs. 7

and 8). On morphological grounds alone, W-cells would be considered a separate neuronal class.

ARE C-LAMINAE W-CELLS A SINGLE CLASS? Rodieck (40) suggested that when applied to retinal ganglion cells, the term W-cell has come to mean any ganglion cell that is neither an X- nor a Y-cell (see also Ref. 42) and that these W-cells actually constitute several distinct classes. However, retrograde labeling experiments (35) indicate that a fairly homogeneous morphological class of retinal ganglion cells projects to the parvocellular C-laminae of the lateral geniculate nucleus, raising the possibility that these specific retinal W-cells and their geniculate target neurons are a single class.

For these reasons we are concerned with the issue of how many cell classes are represented by neurons in the C-laminae, exclusive of the Y-cells found in the dorsal tier of lamina C. We refer to these cells in this paper as W-cells. The morphological and physiological evidence available (this paper; Refs. 5, 23, 49, 53) indicate a fairly wide range of properties for these neurons. However, with one possible exception noted below, the evidence suggests a single class with considerable variability rather than separate classes. For instance, none of the parametric data regarding soma size or dendritic extent (see Figs. 3, 6–8) show evidence of clustering; instead, these parameters apparently vary along a single continuum. Likewise, responsiveness and receptive-field size seem to vary continuously among these neurons (see also Ref. 49).

The one exception noted above refers to response linearity of spatial and temporal summation. Sur and Sherman (49) noted that some of these W-cells respond linearly to counterphased, sine-wave gratings, while others respond nonlinearly. However, these authors noted no other receptive-field differences between linear and nonlinear W-cells and thus suggested that this measure of response linearity may not be sufficient to establish separate cell classes. Indeed, it has not yet been rigorously demonstrated whether or not the parameter of linearity versus nonlinearity is distributed along a continuum for W-cells, whereas such an analysis for X- and Y-cells clearly indicates a bimodal distribu-

tion (24). That is, the identification of linear and nonlinear cells may represent different ends of a continuum. In any case, we found no evidence in the present study of any morphological difference between linear and nonlinear W-cells, although our data are limited to six neurons identified as linear and two as nonlinear.

The issue of classification is far from settled, and clearly more parametric data are needed. However, our tentative conclusion based on the available evidence is that W-cells in the C-laminae constitute a single neuronal class with considerable morphological and physiological variability. In general, we cannot account for this variability and have not seen any clear relationship between the variability of morphological and physiological parameters.

#### *Morphology of dendrites*

INDIVIDUAL DENDRITES. Because so many W-cell dendrites had variable diameters due to numerous swellings (see Fig. 5), we made no attempt to measure these diameters precisely. Our qualitative assessment is that, on average, they are roughly as thin as X-cell dendrites and noticeably thinner than Y-cell dendrites. Among W-cell dendrites commonly seen in our sample are fairly smooth (i.e., appendage free) dendrites, varicose dendrites, beaded dendrites, dendrites with complex appendages distributed both near and far from branch points, and dendrites with appendages clustered near branch points.

These dendritic features have been prominent in cell classification of Golgi-impregnated neurons in the A-laminae: class 1 cells have relatively smooth dendrites, class 2 cells have clustered appendages at dendritic branch points, class 3 cells have complex appendages all along their dendrites, and class 5 cells have varicose or beaded dendrites (11, 19, 51). We reiterate that although the W-cells of our sample most closely correspond to class 4 cells of Golgi-impregnated material (19), they have all of these dendritic features seen in other cell types. Since these features have also been recognized in our population of X- and Y-cells (14), they are obviously not diagnostic for any functional class. As an example of this point, Fig. 17 shows comparisons of grapelike clusters appended at a dendritic branch point for a W-cell (Fig.

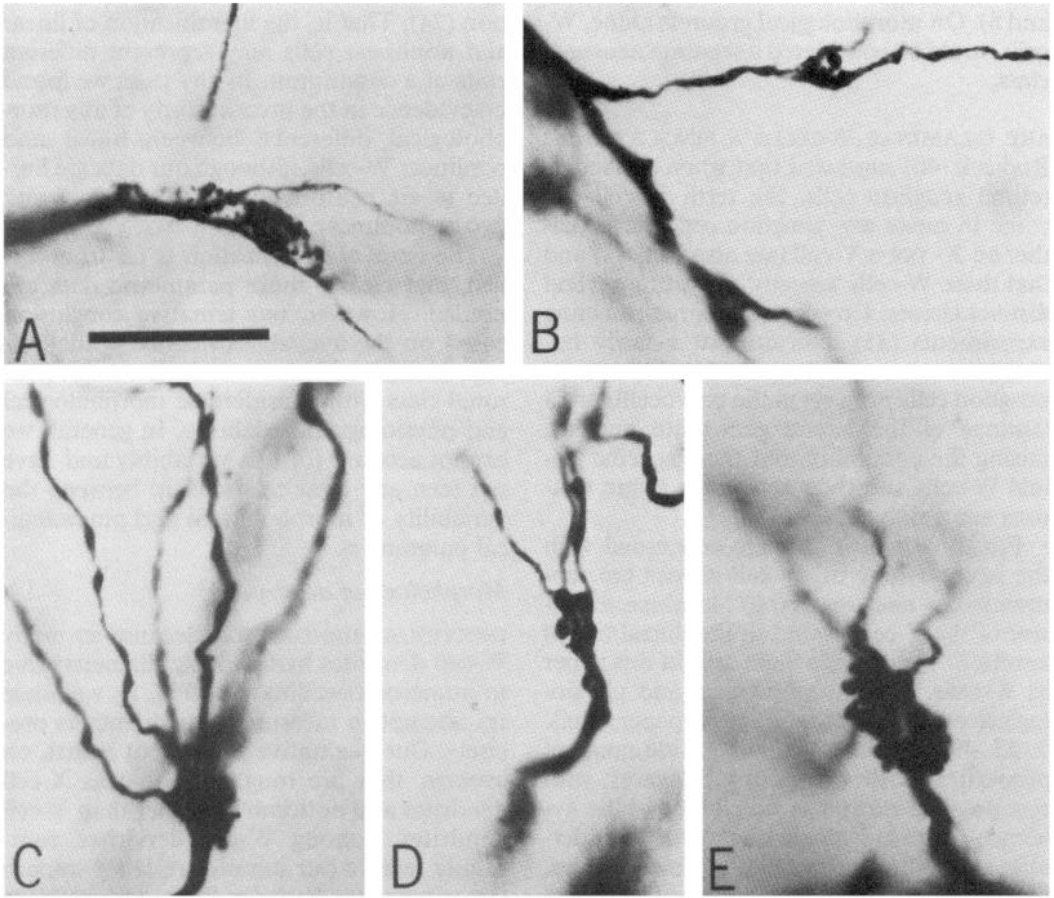


FIG. 17. Photographs of representative appendages clustered at dendritic branch points for geniculate neurons. The scale in *A* is 20  $\mu\text{m}$  and applies as well to *B-E*. *A*: W-cell also illustrated in Figs. 2*B* and 5*C*. *B*: Y-cell in lamina A. *C*: X-cell in lamina A. *D*: X-cell in lamina A1. *E*: Y-cell in lamina A1.

17*A*), two X-cells (Fig. 17*C, D*), and two Y-cells (Fig. 17*B, E*). We still do not know what functional significance, if any, to attribute to this variation in morphology of W-cells, but similar variability seems to be found in a wide range of other geniculate morphological and physiological classes.

**DENDRITIC ARBORS.** Figure 18, which shows a representative example of a W-, X-, and Y-cell, illustrates many of the morphological differences among these cell classes (see also Ref. 14). W-cell and X-cell dendrites are thinner than those of Y-cells. All dendrites of every X-cell are confined to a single lamina, whereas every W- and Y-cell has at least some dendrites that cross laminar borders. However, the most striking difference be-

tween these classes is the geometry of the dendritic arbors. Y-cell arbors are more or less spherical, X-cell dendrites are elongated in a cylinder oriented perpendicular to the laminae, and W-cell dendrites are elongated in a disk oriented parallel to the laminae.

#### *Functional significance of dendritic morphology*

**INDIVIDUAL DENDRITES.** As noted above, W-cell dendrites and X-cell dendrites are roughly comparable in thickness and both are noticeably thinner than Y-cell dendrites. Although the higher synaptic input impedance of a thinner dendrite would be expected to result in a larger postsynaptic potential at the synaptic site for equal amounts of synaptic current, this potential would be more

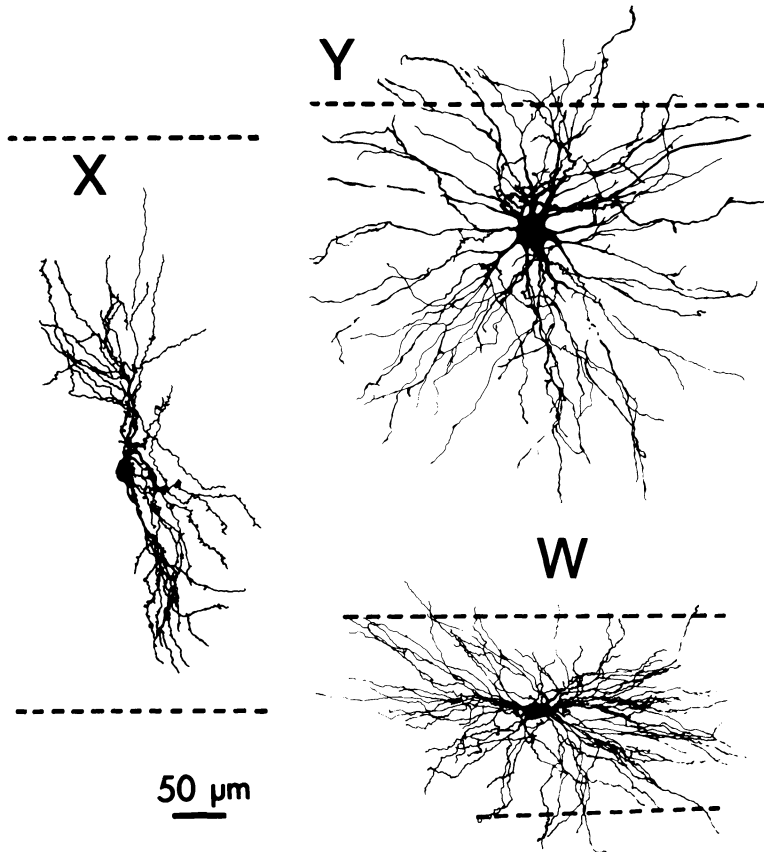


FIG. 18. Camera lucida drawings of a W-cell, X-cell, and Y-cell at the same scale for comparison. Laminar borders are indicated by dashed lines. These cells typify many of the morphological differences among classes. The W-cell is located in lamina C2 and/or C3. Some of its dendrites extend ventrally into the optic tract and others extend dorsally into lamina C1. Its soma is small, its dendrites are thin and varicose, and its dendritic arbor is elongated parallel to the laminar borders. The X-cell soma is located in lamina A1, and its dendrites are entirely confined to that lamina. Its soma is small, its dendrites are thin and have numerous complex, stalked appendages, and its dendritic arbor is elongated perpendicular to the laminar borders. The Y-cell soma is located in lamina A1, and some of its dendrites extend dorsally into lamina A. Its soma is large, its dendrites are thick and have few spinelike appendages, and its dendritic arbor is fairly spherical in shape. For further details, see the text and Ref. 14.

greatly attenuated during electrotonic conduction along the thinner dendrite to the soma and axon hillock (28, 38, 39). As Rall and Rinzel (39) point out, the expected result is a smaller postsynaptic potential measured at the soma of the cell with the thinner dendrites. Furthermore, many X- and some W-cell dendrites have stalked appendages, which, at least for X-cells, are usually postsynaptic sites (52); such appendages are relatively rare for Y-cells. These appendages may act as high-input-impedance paths for electrotonic conduction, which would further attenuate the postsynaptic potentials (7, 38, 39). Ap-

pendage-free W-cell dendrites typically are varicose or beaded (see Table 1), and the conspicuous constrictions, like those of the appendages, are likely to be sites of significant attenuation of postsynaptic potentials. Since there is little overall difference among W-, X-, and Y-cells either in the overall extent of dendrites (Fig. 6) or in their distribution as a function of distance from the soma (Fig. 9A), it seems likely from these differences in thickness and appendages that the dendritic arbor of a Y-cell is better suited to more effective conduction of postsynaptic potentials to the axon hillock than is the arbor of a W-

or X-cell. (An important factor in differential efficiency of signal transmission through W-, X-, and Y-cells is the potentially different thresholds of their axon hillocks, but we cannot yet estimate these values.) The speculations outlined above assume that the dendrites conduct electrotonically so that cable theory can be applied to them (28, 38, 39). Recent descriptions of voltage-dependent, calcium-based action potentials among dendrites of some neurons (37, 54) raise questions about the validity of this assumption.

Contrary to the above speculations, studies of spinal motoneurons (4) suggest that smaller neurons (i.e., analogous to W- and X-cells) are more readily excited by their synaptic inputs than are larger neurons (i.e., analogous to Y-cells). It is not clear for motoneurons whether this reflects a difference between larger and smaller neurons or a difference in their synaptic inputs. Nonetheless, the speculations outlined above are consistent with the observation that geniculate Y-cells seem more responsive than either W- or X-cells to electrical stimulation of the optic chiasm (unpublished observations; Refs. 25, 49, 53). Also, geniculate Y-cells are more responsive to visual stimuli than are W- or X-cells (3, 49), although it is not clear to what extent this difference is already present in the retina. Likewise, while the morphological features we described may contribute to these differences in synaptic transfer functions of W-, X-, and Y-cells, there are many other plausible explanations for these physiological differences.

**DENDRITIC ARBORS.** It seems likely that the difference in the shape of dendritic arbors seen for W-, X-, and Y-cells is also of functional significance. These shapes almost certainly relate to the spatial distribution of the neuron's synaptic inputs, including retinal and nonretinal sources. Whether the geometry of the arbor is determined by the geometry of synaptic inputs or vice versa must remain an open question. In any case, the two most obvious factors of geniculate anatomy to which dendritic geometry probably relates are the lamination and the projection lines (43) that run perpendicular to and through the laminae. Each projection line represents a single point in visual space, and the precise retinotopic map evident in the

lateral geniculate nucleus requires that nearby projection lines map nearby points. Given these factors, the following speculations concerning dendritic geometry seem plausible.

*W-cells.* Since W-cell dendrites are spread out in a fairly thin disk oriented parallel to the laminae, these dendrites cut across the retinotopic map and extend minimally across the laminae. This raises the possibility that the dendrites are organized to receive convergent input from a maximum representation of visual space and/or to obtain maximum input within one of the rather thin C-laminae. While the latter factor may be important to ocular dominance, it is clear that W-cell dendrites do not rigorously obey laminar boundaries (cf. Figs. 10–13).

It is difficult to propose a specific role for the W-cell pathway. A background role is suggested by the poor responsiveness plus diffuse and large receptive fields of W-cells (49). We must emphasize, however, the possibilities that the stimuli or illumination conditions employed by us and others to study these cells may be inadequate to activate them effectively and that the W-cell pathway may be particularly sensitive to the physiological and pharmacological manipulations used in the recording sessions. This qualification notwithstanding, it is obvious that the properties described for W-cells place relatively little emphasis on precise retinotopic mapping and, indeed, may require these neurons to receive afferents across a fairly large representation of visual space.

*X-cells.* X-cell dendrites tend to concentrate near a single projection line. This permits the maximum convergence of synaptic input from the minimum representation of visual space. Because of the relative thickness of the A-laminae, an X-cell can and does have its dendrites contained within a single lamina despite the dendritic orientation along projection lines.

X-cells are the most sensitive to higher spatial frequencies that subservise high spatial resolution and spatial phase (or position) sensitivity. It has been suggested that the X-cell pathway adds spatial detail to and raises acuity from the basic form analysis performed by the Y-cell pathway (31, 32, 44). Spatial resolution and phase sensitivity place a premium on precise retinotopic mapping,

and this may be the significance of the shape of X-cell dendritic arbors.

*Y-cells.* Y-cell arbors exhibit relatively good spherical symmetry. It seems reasonable to assume that spherically asymmetrical arbors are the result of functional pressures that shape the arbors (e.g., such as the requirement to receive synaptic inputs along projection lines or across the retinotopic map, as suggested above). Presumably, such pressures on the morphological development of Y-cells are minimal.

Y-cells are the most sensitive to lower spatial frequencies (32, 49), and this sensitivity is consistent with their proposed major role in basic form analysis (31, 32, 44). Perhaps because these neurons are less concerned with higher spatial frequencies and spatial phase sensitivity, there is no need to concentrate dendrites near a single projection line, but their importance to form analysis dictates against an extreme elongation across projection lines. Indeed, the superior responsiveness of these cells to synaptic input may preclude the need to extend dendrites far in any direction to obtain sufficient synaptic input, and this responsiveness is well suited for a pathway involved in basic form analysis. With no other powerful pressures to create a spherically asymmetric dendritic arbor, the symmetrical arbors of Y-cells are readily explicable.

### *Morphology of somata*

**CORRELATES OF SOMA SIZE.** W-cell somata are slightly (but perhaps not significantly) smaller than X-cell somata, and both classes have distinctly smaller somata than do Y-cells. At least two factors seem to control soma size. One seems to be the extent of the dendritic arbor, since, as Fig. 6 shows, dendritic extent within each of the W-, X-, or Y-cell classes correlates well with soma size. This correlation is most apparent within a class, because if all cells are pooled, the correlation between these parameters is much weaker. Indeed, W-cells, which possess the smallest somata, have the most extensive dendritic arbors (Figs. 3, 5, 6).

This suggests that at least one other factor must combine with dendritic extent to determine soma size. A frequently suggested factor is the number of synaptic terminals or

the extent of the preterminal arbor supported by the neuron in question (20, 34). By this reasoning, geniculate Y-cells have larger somata than do X-cells because a Y-cell's geniculocortical projections are larger than those of an X-cell (13, 16, 17, 26, 47). If true, this would predict that the terminal extent of axons from C-laminae W-cells are significantly smaller than are those of Y-cells and possibly also X-cells. This hypothesis could be tested by HRP injections into physiologically identified W-, X-, and Y-cell axons in the optic radiations.

### **ELECTRODE SAMPLING AMONG SOMATA.**

Electrode sampling should depend on the size of the extracellular zone in which current flow caused by the cell's firing is greater than some threshold value for detection by the electrode. It has often been assumed that electrode sampling characteristics are strongly determined by soma volume (cf. Ref. 27), presumably because a larger soma corresponds to a larger zone of threshold current flow. We recently tested this assumption for X- and Y-cells of the A-laminae and found, surprisingly, that these neurons were sampled electrophysiologically without bias based on soma size, although other factors contributing to electrode sampling, such as responsiveness or dendritic morphology, could not be ruled out (14).

The present study indirectly extends this conclusion to W-cells of the C-laminae, since the soma size distribution of recovered W-cells closely matched that of the available sample (see Fig. 4). Furthermore, we converted the available distribution of Nissl-stained neurons to an expected distribution of recorded neurons by an algorithm whereby the probability of recording was determined by soma volume; we assumed that the cross-sectional area was  $\pi r^2$  and calculated volume as  $4/3\pi r^3$  (see Ref. 14 for a discussion of this algorithm). We found that the observed distribution of recorded W-cells did not differ from the available (Nissl stained) distribution but did differ from the distribution expected on the basis of soma volume ( $P > 0.1$  and  $< 0.05$ , respectively). The same relationships held for X- and Y-cells of the A-laminae (14). Thus the ability to record, impale, inject with HRP, and recover a W-cell is not demonstrably related to its soma size. Except for the

unlikely possibility that recorded cells with larger somata are somehow systematically excluded from the sample of recovered neurons, these data indicate little effect of electrode sampling based on soma size. The conclusion that three such distinct neuronal populations, geniculate W-, X-, and Y-cells, should exhibit the same lack of strong electrode sampling bias related to soma size should raise a serious doubt about the general validity of this assumption.

#### *Morphology of axons*

**AXON DIAMETER.** We have suggested earlier for geniculate X- and Y-cells that axonal diameter may be related to the extent of terminals in cortex: a thicker axon is necessary to permit transport of the necessary metabolic products needed to maintain a larger or more active terminal arbor (14). This reasoning suggests that thinner axons are associated with smaller or less metabolically active terminal fields. Furthermore, other factors often associated with axon diameter (e.g., conduction velocity) may be epiphenomena of the terminal field's metabolic requirements. Since W-cell axons are significantly thinner than X- or Y-cell axons, this predicts that W-cell axons should form smaller or less metabolically active terminal fields in cortex than do X- or Y-cell axons. Thus a consideration of either the relationship between soma size and dendritic extent (described above) or axon diameter leads to the same testable prediction.

**AXON COLLATERALS.** Most Y-cells and some X-cells emit axon collaterals from their parent axons as they pass through the perigeniculate nucleus just dorsal to lamina A. This perigeniculate innervation is thought to be part of an inhibitory feedback loop whereby perigeniculate cells give rise to axons that richly innervate the geniculate laminae (9, 14, 36). It is not clear to what extent individual perigeniculate neurons receive input from one or more of these pathways, although Dubin and Cleland (9) reported that many of these cells received convergent X- and Y-cell input. Our data make it clear that most W-cells also innervate the perigeniculate nucleus via axon collaterals.

Perhaps more interesting but less common than perigeniculate collaterals are collateral branches that innervate the main laminae of

the lateral geniculate nucleus (i.e., intrageniculate collaterals). Previously, we noted that a distinct minority of both X- and Y-cells display such collaterals (14). In the present study, we can extend this observation to include 2 of 16 W-cells with filled axons. While relatively rare, these collaterals raise the possibility that many responses disynaptic to electrical stimulation of the optic chiasm could arise from axon collaterals of relay cells rather than from axons of interneurons that receive optic tract input (but see Ref. 36).

We may have actually underestimated the number of these perigeniculate and intrageniculate axon collaterals due to their extremely slender appearance, particularly for W- and X-cells. These collaterals are often so fine that they approach the detection limit with the light microscope. Many more may have been present but missed. We thus feel that our evidence of axon collaterals should be viewed as a conservative estimate of the importance of these pathways to geniculate circuitry.

#### *Concluding remarks*

Two main conclusions may be drawn from this study plus our previous one (14). First, the morphological features of W-, X-, and Y-cells are quite distinct from one another. These morphological differences almost certainly relate to functional differences in the circuits of each pathway. Thus, functional differences in these pathways are not limited to retinal circuitry and simply relayed to cortex via the lateral geniculate nucleus. Instead, differences seem to be amplified by geniculate circuitry. We have described above how differences in the morphology of dendrites and shape of dendritic arbors might contribute to the different functional roles of the W-, X-, and Y-cell pathways. Differences in dendritic morphology may contribute to the more reliable synaptic transmission through the Y-cell pathway than through either the W- or X-cell pathways. Furthermore, W-cell dendritic arbors suggest convergence of inputs from a large retinotopic region for diffuse processing of visual signals, X-cell arbors seem to place a premium on receiving inputs from a limited retinotopic locale, and Y-cell arbors are best suited for reliable transmission of the crucial lower spatial frequencies.

The second general conclusion is that W-cells of the C-laminae form a single neuronal class that is quite distinct from geniculate X- and Y-cells and that includes considerable morphological and physiological variability. We cannot account for this variability, but it seems to reflect a continuum of physiological and morphological characteristics rather than distinct classes.

## ACKNOWLEDGMENTS

We gratefully acknowledge the expert technical assistance of Sally Gibson and Joan Sommermeyer.

## REFERENCES

- ADAMS, J. C. Technical considerations on the use of horseradish peroxidase as a neuronal marker. *Neuroscience* 2: 141-145, 1977.
- BISHOP, P. O., BURKE, W., AND DAVIS, R. Single unit recording from antidromically activated optic radiation neurones. *J. Physiol. London* 162: 432-450, 1962.
- BULLIER, J. AND NORTON, T. T. Comparison of receptive-field properties of X and Y ganglion cells with X and Y lateral geniculate cells in the cat. *J. Neurophysiol.* 42: 274-291, 1979.
- BURKE, R. E. AND RUDOMÍN, P. Spinal neurons and synapses. In: *Handbook of Physiology. The Nervous System*. Bethesda, MD: Am. Physiol. Soc., 1977, sect. 1, vol. 1, part 2, chapt. 24, p. 877-944.
- CLELAND, B. G., MORSTYN, R., WAGNER, H. G., AND LEVICK, W. R. Long-latency retinal input to lateral geniculate neurones of the cat. *Brain Res.* 91: 306-310, 1975.
- COWAN, W. M., GOTTLIEB, D. I., HENDRICKSON, A. E., PRICE, J. L., AND WOOLSEY, T. A. The autoradiographic demonstration of axonal connections in the central nervous system. *Brain Res.* 37: 21-51, 1972.
- DIAMOND, J., GRAY, E. G., AND YASARGIL, G. M. The function of the dendritic spine: a hypothesis. In: *Excitatory Synaptic Mechanisms*, edited by P. Andersen and J. K. S. Jansen. Oslo: Scandinavian University, 1970, p. 213-222.
- DREHER, B. AND SEFTON, A. J. Properties of neurons in cat's dorsal lateral geniculate nucleus: a comparison between medial interlaminar and laminated parts of the nucleus. *J. Comp. Neurol.* 183: 47-64, 1979.
- DUBIN, M. W. AND CLELAND, B. G. Organization of visual inputs to interneurons of lateral geniculate nucleus of the cat. *J. Neurophysiol.* 40: 410-427, 1977.
- ENROTH-CUGELL, C. AND ROBSON, J. G. The contrast sensitivity of retinal ganglion cells of the cat. *J. Physiol. London* 187: 517-552, 1966.
- FAMIGLIETTI, E. V. Dendro-dendritic synapses in the lateral geniculate nucleus of the cat. *Brain Res.* 20: 181-191, 1970.
- FERNALD, R. AND CHASE, R. An improved method for plotting retinal landmarks and focusing the eyes. *Vision Res.* 11: 95-96, 1971.
- FERSTER, D. AND LEVAY, L. The axonal arborizations of lateral geniculate neurons in the striate cortex of the cat. *J. Comp. Neurol.* 182: 923-944, 1978.
- FRIEDLANDER, M. J., LIN, C.-S., STANFORD, L. R., AND SHERMAN, S. M. Morphology of functionally identified neurons in the lateral geniculate nucleus of the cat. *J. Neurophysiol.* 46: 80-129, 1981.
- FRIEDLANDER, M. J., LIN, C.-S., AND SHERMAN, S. M. Structure of physiologically identified X and Y cells in the cat's lateral geniculate nucleus. *Science* 204: 1114-1117, 1979.
- GEISERT, E. E. Cortical projections of the lateral geniculate nucleus in the cat. *J. Comp. Neurol.* 190: 793-812, 1980.
- GILBERT, C. D. AND WIESEL, T. N. Morphology and intracortical projections of functionally characterized neurones in the cat visual cortex. *Nature London* 280: 120-125, 1979.
- GRAYBIEL, A. M. AND BERSON, D. M. Autoradiographic evidence for a projection from the pretectal nucleus of the optic tract to the dorsal lateral geniculate complex in the cat. *Brain Res.* 195: 1-12, 1980.
- GUILLERY, R. W. A study of Golgi preparations from the dorsal lateral geniculate nucleus of the adult cat. *J. Comp. Neurol.* 128: 21-50, 1966.
- GUILLERY, R. W. Binocular competition in the control of geniculate cell growth. *J. Comp. Neurol.* 144: 117-130, 1972.
- GUILLERY, R. W. AND SCOTT, G. L. Observations on synaptic patterns in the dorsal lateral geniculate nucleus of the cat: the C laminae and the perikaryal synapses. *Exp. Brain Res.* 12: 184-203, 1971.
- HICKEY, T. L. AND GUILLERY, R. W. An autoradiographic study of retinogeniculate pathways in the cat and the fox. *J. Comp. Neurol.* 156: 239-254, 1974.
- HITCHCOCK, P. F. AND HICKEY, T. L. A study of Golgi impregnated neurons in the C-laminae of the cat's dorsal lateral geniculate nucleus (dLGN). *Invest. Ophthalmol. Visual Sci. Suppl.* 22: 243, 1982.
- HOCHSTEIN, S. AND SHAPLEY, R. M. Quantitative analysis of retinal ganglion cell classifications. *J. Physiol. London* 262: 237-264, 1976.
- HOFFMANN, K.-P., STONE, J., AND SHERMAN, S. M. Relay of receptive-field properties in dorsal

This research was supported by Public Health Service Grant EY03038.

Present address of L. R. Stanford: Dept. of Structural and Functional Sciences, School of Veterinary Medicine, University of Wisconsin, Madison, WI 53715.

Present address of M. J. Friedlander: University of Alabama, Dept. of Physiology and Biophysics, Birmingham, AL 35294.

Address requests for reprints to S. M. Sherman.

Received 6 January 1983; accepted in final form 5 April 1983.

- lateral geniculate nucleus of the cat. *J. Neurophysiol.* 35: 518-531, 1972.
26. HUMPHREY, A. L., SUR, M., AND SHERMAN, S. M. Cortical axonal terminal arborization and soma location of single, functionally identified lateral geniculate nucleus neurons. *Soc. Neurosci. Abstr.* 8: 2, 1982.
  27. HUMPHREY, D. R. AND CORRIE, W. S. Properties of pyramidal tract neuron system within a functionally defined subregion of primate motor cortex. *J. Neurophysiol.* 41: 216-243, 1978.
  28. KOCH, C., POGGIO, T., AND TORRE, V. Retinal ganglion cells: a functional interpretation of dendritic morphology. *Proc. R. Soc. London Ser. B* 298: 227-264, 1982.
  29. KRATZ, K. E., WEBB, S. V., AND SHERMAN, S. M. Studies of the cat's medial interlaminar nucleus: a subdivision of the dorsal lateral geniculate nucleus. *J. Comp. Neurol.* 180: 601-614, 1978.
  30. LAVAIL, J. H., AND LAVAIL, M. M. Retrograde axonal transport in the central nervous system. *Science* 176: 1416-1417, 1972.
  31. LEHMKUHLE, S., KRATZ, K. E., AND SHERMAN, S. M. Spatial and temporal sensitivity of normal and amblyopic cats. *J. Neurophysiol.* 48: 372-387, 1982.
  32. LEHMKUHLE, S., KRATZ, K. E., MANGEL, S. C., AND SHERMAN, S. M. Spatial and temporal sensitivity of X- and Y-cells in dorsal lateral geniculate nucleus of the cat. *J. Neurophysiol.* 43: 520-541, 1980.
  33. LENNIE, P. Parallel visual pathways. *Vision Res.* 20: 561-594, 1980.
  34. LEVAY, S., WIESEL, T. N., AND HUBEL, D. H. The development of ocular dominance columns in normal and visually deprived monkeys. *J. Comp. Neurol.* 191: 1-51, 1980.
  35. LEVENTHAL, A. G. Morphology and distribution of retinal ganglion cells projecting to different layers of the dorsal lateral geniculate nucleus in normal and Siamese cats. *J. Neurosci.* 2: 1024-1042, 1982.
  36. LINDSTROM, S. Synaptic organization of inhibitory pathways to principal cells in the lateral geniculate nucleus of the cat. *Brain Res.* 234: 447-453, 1982.
  37. LLINÁS, R. AND SUGIMORI, M. Calcium conductances in Purkinje cell dendrites: their role in development and integration. *Prog. Brain Res.* 51: 323-334, 1979.
  38. RALL, W. Core conductor theory and cable properties of neurons. In: *Handbook of Physiology. The Nervous System*. Bethesda, MD: Am. Physiol. Soc., 1977, sect. 1, vol. 1, part 1, chapt. 3, p. 39-97.
  39. RALL, W. AND RINZEL, J. Branch input resistance and steady attenuation for input to one branch of a dendritic neuron model. *Biophys. J.* 13: 648-688, 1973.
  40. RODIECK, R. W. Visual pathways. *Annu. Rev. Neurosci.* 2: 193-225, 1979.
  41. ROWE, M. H. AND STONE, J. Naming of neurones. *Brain Behav. Evol.* 14: 185-216, 1977.
  42. ROWE, M. H. AND STONE, J. The interpretation of variation in the classification of nerve cells. *Brain Behav. Evol.* 17: 123-151, 1980.
  43. SANDERSON, K. J. The projection of the visual field to the lateral geniculate and medial interlaminar nuclei in the cat. *J. Comp. Neurol.* 143: 101-118, 1971.
  44. SHERMAN, S. M. Parallel pathways in the cat's geniculocortical system: W-, X-, and Y-cells. In: *Changing Concepts in the Nervous System*, edited by A. Morrison and P. Strick. New York, Academic, 1982, p. 337-359.
  45. SHERMAN, S. M. AND SPEAR, P. D. Organization of the visual pathways in normal and visually deprived cats. *Physiol. Rev.* 62: 738-855, 1982.
  46. STANFORD, L. R., FRIEDLANDER, M. J., AND SHERMAN, S. M. Morphology of physiologically identified W-cells in the C laminae of the cat's lateral geniculate nucleus. *J. Neurosci.* 1: 578-584, 1981.
  47. STONE, J. AND DREHER, B. Projection of X- and Y-cells of the cat's lateral geniculate nucleus to area 17 and 18 of visual cortex. *J. Neurophysiol.* 36: 551-567, 1973.
  48. STONE, J., DREHER, B., AND LEVENTHAL, A. Hierarchical and parallel mechanisms in the organization of visual cortex. *Brain Res. Rev.* 1: 345-394, 1979.
  49. SUR, M. AND SHERMAN, S. M. Linear and nonlinear W-cells in C-laminae of the cat's lateral geniculate nucleus. *J. Neurophysiol.* 47: 869-884, 1982.
  50. TORREALBA, F., PARTLOW, G. D., AND GUILLERY, R. W. Organization of the projection from the superior colliculus to the dorsal lateral geniculate nucleus of the cat. *Neuroscience* 6: 1341-1360, 1981.
  51. UPDYKE, B. V. A Golgi study of the class V cell in the visual thalamus of the cat. *J. Comp. Neurol.* 186: 603-620, 1979.
  52. WILSON, J. R., FRIEDLANDER, M. J., AND SHERMAN, S. M. Synaptic morphology of X- and Y-cells in the cat's dorsal lateral geniculate nucleus. *Soc. Neurosci. Abstr.* 6: 583, 1980.
  53. WILSON, P. D., ROWE, M. H., AND STONE, J. Properties of relay cells in the cat's lateral geniculate nucleus. A comparison of W-cells with X- and Y-cells. *J. Neurophysiol.* 39: 1193-1209, 1976.
  54. WONG, R. K. S., PRINCE, D. A., AND BASBAUM, A. I. Intradendritic recordings from hippocampal neurons. *Proc. Natl. Acad. Sci. USA* 76: 986-990, 1979.